Marine Geology
November 2022, Volume 453, Pages 106922 (19p.)
https://doi.org/10.1016/j.margeo.2022.106922
https://archimer.ifremer.fr/doc/00798/90964/

Planktic-benthic foraminifera ratio (%P) as a tool for the reconstruction of paleobathymetry and geohazard: A case study from Taiwan

Tapia Raúl [1, *], Le Sicheng [1], Ho Sze Ling [1], Bassetti Maria-Angela [2], Lin In-Tian [3], Lin Hui-Ling [4], Chang Yuan-Pin [4], Jiann Kuo-Tung [4], Wang Pei-Ling [1], Lin Jheng-Kuan [1], Babonneau Nathalie [5], Ratzov Gueorgui [6], Hsu Shu-Kun [7], Su Chih-Chieh [1]

[1] Institute of Oceanography, National Taiwan University, No. 1, Sec. 4, Roosevelt Road, 10617 Taipei, Taiwan
[2] CEFREM-UMR 5110, Université de Perpignan Via Domitia, 52 Avenue Paul Alduy, 66860 Perpignan, cedex, France
[3] Exploration and Development Research Institute, CPC Corporation, Miaoli 36042, Taiwan
[4] Department of Oceanography, National Sun Yat-sen University, Kaohsiung 80424, Taiwan
[5] Geo-Ocean, UMR6538 CNRS-UBO-Ifremer-UBS, IUEM, Plouzané, France
[6] Université Côte d'Azur, CNRS, Observatoire de la Côte d'Azur, IRD, Géoazur, Nice, France
[7] Department of Earth Sciences, National Central University, Taiwan

* Corresponding author : Raul Tapia, email address : raultapia@ntu.edu.tw

Abstract :

The calcite tests of foraminifera are an important biogenic component of marine sediments. The abundance of foraminiferal tests in marine sediments broadly varies with bathymetry, thus has been used to reconstruct paleobathymetry. It is also promising as a tracer for downslope transport triggered by earthquakes and typhoons, especially if the displaced material from shallow locality contrasts strongly with the background autochthonous sediments in terms of foraminiferal abundance, such as the ratio of benthic and planktic foraminifera termed %P. However, its applicability in sediments off Taiwan has not been assessed. Taiwan is located in the path of typhoons and at tectonic plate margins, where typhoons and earthquakes may trigger submarine geohazards. This, combined with the fact that its seafloor spans a large bathymetric range, render this region an ideal natural laboratory to evaluate the applicability of %P as a proxy for tracing submarine geohazards and bathymetry. Here we report foraminiferal abundance, %P, grain size and elemental data from 148 surface sediment samples off 6 sectors off Taiwan, namely Southern Okinawa Trough, Hoping-Nanao-Hateruma Basins, Taitung-Hualien, Hengchun Ridge, Gaoping, and Changyun Sand Ridge. Of all the hydrographic and sedimentological parameters assessed, seafloor bathymetry is the major driver of foraminiferal abundance and %P in these regions. Notably, several data points deviate from the regional %P-water depth relationship. Based on sedimentological parameters and previous studies, we posit that these outliers may have to do with local sedimentation setting. These processes include earthquake-induced sediment transport via submarine canyon in the Southern Okinawa Trough, typhoon-triggered sediment flushing in Gaoping Canyon, cross-shelf and northward advection of planktic foraminifera on the Gaoping shelf, and carbonate dissolution in the deep Hateruma Basin. Off Taiwan, the %P value in sediments increases exponentially with bathymetry ($R2 = 0.72$, $n = 81$), and agrees well with the global calibration obtained by combining data from several

regions of the global ocean (R2 = 0.86, n = 1004). The regional %P-water depth relationship may be useful for reconstructing paleobathymetry here, albeit with an uncertainty in the range of 14–1600 m. The uncertainty increases with water depth. Our results also highlight the potential of the %P index as a tracer for downslope transport and lateral advection in the water column. In conclusion, the downcore application of %P has the potential to reconstruct past geohazard events while also identifying autochthonous sediment sequences that are suitable for paleoceanographic reconstruction.

Highlights

► Foraminifera, grain size, TOC, and C/N data of 148 core-tops off Taiwan. ► Bathymetry is the main driver of foraminiferal abundance. ► Planktic foraminifera percentage (%P) is strongly correlated with seafloor bathymetry. ► Lateral advection, carbonate dissolution, and downslope sediment transport affect %P. ► %P a promising tool for paleo-bathymetry, −geohazard and -oceanography studies.

Keywords : Foraminifera, %P, paleobathymetry, downslope sediment transport, geohazard, Taiwan

INTRODUCTION

The calcite tests of foraminifera are a major biogenic component of marine sediments. The displacement of foraminiferal tests after deposition may occur as an outcome of submarine sediment density flow events such as turbidity currents, debris flows, hyperpycnal plumes, and submarine landslides (Schmuker, 2000). Thus, the study of foraminiferal tests in sediments, alongside grain size, mineral composition, and organic carbon content analysis, are the primary tools in the identification of mass sediment transport events in the sedimentary record (Jones, 2013). The aforementioned approaches are highly complementary. Although they can be applied separately, when used in tandem they afford a more comprehensive picture of the sedimentation process.

Contrasting displaced foraminifera with modern autochthonous fauna allows the identification of the sedimentary source (original depth of deposition) and the inference of transport processes (Ash-Mor et al., 2017; Ash-Mor et al., 2021; Usami et al., 2017). The inclusion of gravitationally displaced individuals (i.e., allochthonous fauna) in the autochthonous foraminiferal assemblage from deeper parts of the basins will alter the diversity and dominance parameters of the local fauna (Hayward et al., 2019; Schröder-Adams et al., 2008). In general, during highly dynamic downslope transport, foraminiferal tests can be subjected to size sorting, abrasion, fragmentation, or dissolution (thinner shelled calcareous tests) when deposited close to or below the calcite compensation depth (Hayward et al., 2019; Schröder-Adams et al., 2008; Sugawara et al., 2009; Uchida et al., 2010). However, these features may vary depending on the specific characteristics of the gravity flow (e.g., Usami et al., 2017; Usami et al., 2021). These changes in foraminiferal parameters caused by sediment transport may thus complement the information obtained from traditional sedimentological approaches. In fact, the percentage of planktic foraminifera (%P) has been used to trace turbidites and other types of debris flows, as well as paleobathymetric reconstructions in deep geological time (Hayward et al., 2019; Jones, 2013). In contrast to mineralogical composition and grain size approaches where the observed data are driven exclusively by physical or chemical processes, the use of foraminifera to interpret sediment transport processes requires additional considerations, as environmental parameters

may also influence foraminiferal distribution (van der Zwaan et al., 1990). Therefore, understanding the living environmental conditions of the organism and their modern distribution in sediments is a prerequisite to downcore applications (Gooday, 2003; Jones, 2013; van der Zwaan et al., 1999).

Taiwan is prone to natural geohazards linked to climate (e.g., tropical cyclones) and tectonics (e.g., earthquakes). These so-called extreme events can cause enormous damage to public infrastructure, private property, and fatalities. A less recognized aftershock of these natural hazards is their ability to generate turbidity currents and gravity flows on the seafloor. Therefore, Taiwan is an ideal natural laboratory to study the impact of submarine sediment density flows on the distribution of foraminiferal tests in sediments.

To date, foraminiferal studies off Taiwan have been mostly focusing on the temporal flux in the water column (i.e., sediment traps), benthic foraminiferal biocenosis (Lin and Hsieh, 2007; Lin, 2014; Lin et al., 2011), and the application of benthic foraminifera to assess coral reef health (Chen and Lin, 2017). Little attention has been paid to the utility of foraminifera as a tracer for geohazards or extreme events, despite promising early observations that suggested a correlation between the transport of foraminiferal tests and the landfall of typhoons (Lin et al., 2005).

The main objective of this study is to assess the applicability of foraminiferal indices, with emphasis on %P, as a tracer of sediment transport in response to extreme events such as typhoons and earthquakes. To this end, we mapped the spatial distribution of foraminiferal indices in surface sediments off Taiwan spanning a large bathymetric range (Fig. 1a). Our approach is based on the ecology of foraminifera, that is, the relationship between bathymetry and the distribution of planktic and benthic foraminifera (Berger and Diester-Haass, 1988; Gibson, 1989; Hayward and Triggs, 2016; Hayward et al., 2019; Jones, 2013; Nigam and Henriques, 1992; Schmuker, 2000; van der Zwaan et al., 1999, 1990; van Hinsbergen et al., 2005). This approach implies that deviations from the main bathymetry-foraminifera relationship reflect “anomalies” in the depositional environment due to processes like downslope transport of sediment. Whilst seemingly straightforward, the accuracy of this approach requires further scrutiny as this relationship varies from region-to-region (van der Zwaan et al., 1990). To better

constrain the bathymetry-foraminifera relationship off Taiwan, we used grain size and organic carbon content to cross-evaluate the likelihood that the collected sediments have been tampered by sediment transport processes. We also assessed if the foraminiferal indices in our study region change in response to environmental parameters other than water depth, e.g., seawater temperature, salinity, and water fertility.

1.1 Modern climate, oceanography and geological setting of study area

The upper ocean circulation around Taiwan is dominated by the warm Kuroshio Current that originates in the equatorial Pacific. At the Luzon Strait, a minor branch of this nutrient-deficient current splits in the direction of the South China Sea and flows along the southern part of Taiwan toward the Taiwan Strait (Fig. 1b). The upper circulation in the Taiwan Strait is primarily controlled by the Taiwan Warm Current, which consists of waters from the South China Sea and the Kuroshio branch, and flows towards the East China Sea all year round. In winter, the East China Sea Coastal Current (ECSCC) flowing towards the South China Sea can be observed in the Taiwan Strait (Fig. 1b) (Huang et al., 2015; Liang et al., 2003). The main branch of the Kuroshio Current flows northward along the eastern flank off Taiwan, crossing the Ilan Ridge at the Yonaguni Depression toward the East China Sea (Fig. 1b). The continental shelf to the north of the southernmost Okinawa Trough creates a topographic constriction for the Kuroshio Current, prompting the formation of eddies that actively capture and retain suspended sediments on the shelf. The shelf sediments are subsequently delivered downslope into the Okinawa Trough via submarine canyons such as the Mien-Hua Canyon (Fig. 1c) (Chiang et al., 2022), implying the relevance of downslope transport in affecting the sediment composition in the Okinawa Trough sector. Indeed, previous studies have proposed that the carbonate content in the Okinawa Trough is driven mainly by dilution (e.g., Chang et al., 2009) despite the fact that the depth of the Carbonate Compensation Horizon (~1600 - ~1800 m water depth) here is substantially shallower than other areas off Taiwan (Chang et al., 2009; Chen et al., 2006). Taiwan is particularly prone to seismic activity due to its location at the margin of the Philippine Sea and Eurasian plates that collide at a rate of 8 cm yr^{-1} (Lehu et al., 2015; Su et al., 2012).

Although large seismic events have occurred in the central mountain range (i.e., Chi-chi earthquake, 1999), most of the seismic activity concentrates along the eastern coast of Taiwan and along the east-west axis of the Southern Okinawa Trough. In the past 22 years, 23 Mw ≥ 6.5 earthquakes have occurred here (Seismological Center – Republic of China, 2022). Such active seismic activity shapes the seafloor morphology by facilitating the supply of material downslope via gravity flows (Huh et al., 2004; Lee et al., 2004).

In addition, Taiwan is also marked by frequent occurrences of tropical cyclones (known locally as typhoons) (Water Resources Agency – Republic of China, 2022). Although tropical cyclones may occur throughout the year, they are most severe during May to October, which drives a marked seasonality in precipitation patterns as >75 % of annual rainfall, on average >2500 mm y^{-1}, occurs during late summer and early autumn (Water Resources Agency – Republic of China, 2022). Typhoons, usually accompanied by strong winds and heavy rains, can in some cases deliver as much rain as the total amount during a normal year. These short-lived episodes of heavy rain increase runoff and sediment load delivered by the river system to coastal waters around Taiwan (Chien and Kuo, 2011; Lee et al., 2015). For example, the Morakot typhoon (2009) delivered an accumulated 3000 mm of rainfall within a time window of 4 days with a peak of 500 to 800 mm in 24 hours (Chien and Kuo, 2011), which led to over 12000 landslides and extensive flooding in southern Taiwan. As a result of the heavy rains during the Morakot typhoon, a large amount of sediment was removed and transported, leading to the increase in runoff and sediment load of the Gaoping River in southern Taiwan, from its long-term annual averages of <1000 m s^{-1} and ~23 Mt to ranges of 3800–~27000 m s^{-1} and 450–700 Mt (Lee et al., 2015). The excessive discharge of sediment led to the development of several sediment gravity flows that damaged the submarine cables downstream of the Gaoping Submarine Canyon (Su et al., 2012). The Gaoping Submarine Canyon (Fig. 1d) stretches for 260 km covering a bathymetric range from 80 m to 3400 m water depth and serves as a channel to deliver terrigenous materials and carbon into the South China Sea. Substantially smaller, the Fangliao Submarine Canyon stretches for 60 km across the continental slope of the Gaoping

sector and connects with the lower section of the Gaoping Submarine Canyon (Fig. 1d) (Su et al., 2012).

2. MATERIALS AND METHODS

Surface sediment samples (n=148) analyzed in this study (Fig. 1) were collected during several oceanographic cruises carried out between 2002 and 2018 on board of Taiwanese vessels R/Vs Ocean Researcher 1, 2, 3 and New Ocean Researcher 1, as well as French vessel R/V Marion Dufresne. Samples were retrieved using various gears, including sediment grab, box corer, and gravity corer, from water depths ranging from 13 to 5714 m (see Table S1 for details). Most of the surface sediment samples correspond to the upper 2 cm of the sedimentary column except the materials recovered using a sediment grab that integrated the upper 5–8 cm (see Table S1 for details). After recovery, the sediments were refrigerated (4ºC) and sampled in laboratories on land, except for grab samples which were sampled onboard. The use of various sampling gear may cause some scatter in the data set due to the different influences that each gear may have on the uppermost part of the sediment column, especially the unconsolidated flocculent surface layer. However, we considered its effects minimal given the overall high sedimentation rates dominating our study area (see section 4.3.1and Fig. 8), as well as the observations that suggest that in some sectors, the upper ~12 cm of the sedimentary column were deposited between 4 to 6 months (Huh et al., 2009). Study sites were grouped into two main geographical areas, namely (1) East Taiwan (>121º E; n = 85) and (2) West Taiwan (<121º E; n = 63) (Fig. 1a). East Taiwan comprises sites in the Southern Okinawa Trough, Hoping-Nanao-Hateruma Basins, and Taitung-Hualien Slope, while West Taiwan comprises Hengchun Ridge, Changyun Sand Ridge, and Gaoping sector (Fig. 1a).

>> Figure 1<<

2.1 Sediment sample processing

After sampling, surface sediment samples were freeze-dried, weighed, and further subsampled for foraminiferal and geochemical analyses (see Table S1 for details). In the case of insufficient material for both analyses, we prioritized micropaleontological analysis. The subsamples for foraminiferal analysis were wet-sieved through a sieve of 63 µm open mesh, and the remnant was dried at low temperature (50 ºC) and weighed.

2.2 Foraminifera recovery and associated indices

Sediment samples (>63 µm) were dry-sieved through sieves of 125 and 250 µm open mesh. In this study we focus on the >125 µm size fraction. The size fraction of 63–125 µm was not considered in this study because of two reasons. First, as previous work has shown, the faunal composition (e.g., bathymetric group) is similar for the small size fraction (63–125 µm) and the size fraction >125 µm (Hayward et al., 2019). Second, the small size fraction (63–125 µm) usually contains a large proportion of juvenile forms that are problematic to identify, and its recovery is extremely time consuming (Schneider et al., 1987; Schönfeld et al., 2012; Hayward et al., 2019). We acknowledge that the use of the size fraction >125 µm may lead to lower foraminifera counts compared with that of the size fraction >63 µm (see Weinkauf and Milker 2018 and references therein for details) due to the omission of specimens in 63–125 µm. Thus, the census counts based on >125 µm fraction may be underestimated. However, we argue that the size fraction >125 µm represents the best trade-off considering the loss of the faunal inventory and diversity, statistical confidence (census counts from the >63 µm fraction might be compromised due to the high proportion of unidentifiable juveniles) and processing time (Schönfeld et al., 2012; Hayward et al., 2019). To examine whether our results are comparable to studies based on the >63 µm fraction, we compared the results obtained for the >63 µm and >125 µm fractions from a subset of our samples (n = 30). As shown in Fig. 6 and discussed in section 4.1, there is no significant difference in the %P results obtained using these two size fractions.

The census count only considered intact planktic and benthic foraminiferal tests from the size fraction of >125 µm. Our approach was to count at least 300 specimens per sample. In the case wherein the sample contains <300 specimens, we counted all available specimens (Schönfeld et al., 2012; Hayward et al., 2019). %P considers only 2 end members i.e. total planktonic and benthic foraminifera, thus the effective total counts needed may not be as high as for assemblage studies that rely on the statistical significance of the relative abundance of tens of species within the population. The abundance was calculated for each sample and presented as the number of organisms per gram of dry sediment (ind. g^{-1}) for the size fraction of >125 µm. The percentage of planktic foraminifera (%P) is defined as the ratio of planktic foraminiferal tests in the total pool of foraminiferal tests in the sediment, and is calculated as follows:

$$\%P = P / (P+B) * 100$$

where P is the number of specimens of planktic foraminifera and B is the number of specimens of benthic foraminifera. Following Hayward et al (2019), only samples with at least 50 specimens were considered for the calculation of %P.

Our results were compared with several regional %P data sets from the Mediterranean, Atlantic, Indian and Pacific oceans, including Gulf of Maine (Parker 1948), Gulf of Mexico (>114 µm, Parker, 1954), Gulf of California (>62 µm, Uchio 1960), SE Coast of the US (>61 µm, Wilcoxon, 1964), Indonesia (>125 µm, van Marle et al., 1987), India (>63 µm, Nigam and Henriques, 1992), Mediterranean Sea (>125 µm, de Rijk et al., 1999), Caribbean (>150 µm, Schmuker 2000), Okinawa (>125 µm, Koyanagi et al., 2010), and New Zealand (>63 µm, Hayward and Triggs; 2016). PlotDigitizer (https://plotdigitizer.com) was used to digitize three of these data sets, i.e., the data set of Uchio (1960) from Figure 10 of van der Zwaan et al. (1990), the data set of Wilcoxon (1964) from Figure 13 of van der Zwaan et al. (1990), and the data set of Rijk et al. (1999) from the original article.

2.3 Geochemical and sedimentological parameters

2.3.1 Elemental analysis

The Total Organic Carbon (TOC) and Total Nitrogen (TN) contents were measured in three laboratories with slightly different methodologies (details in Table S1). The samples measured in the Institute of Oceanography (NTU) were decalcified using 2N hydrochloric acid (HCl, aq), dried at 50 °C, measured using an Vario MICRO CUBE (Elementar) Elemental Analyzer and calibrated using Soil Calibration Material 502-062 (N: 0.093 %, C : 0.924 %; LECO Corporation).Samples measured in National Sun Yat-sen University were decalcified using phosphoric acid (10%), measured using an Analytic Jena Multi N/C 2100 Elemental Analyzer, and calibrated using pure CaCO3 (C: 12%). The samples measured in the Department of Geoscience (NTU) were decalcified using 3N hydrochloric acid (HCl, aq), freeze-dried, measured using a Flash EA 1112 Elemental Analyzer and calibrated using BBOT standard (6.51% N and 72.53% C) together with an in-house standard (N: 0.06% and C: 0.5%). The overall relative error of TOC and TN measurements was less than 5% based on replicate analysis. The C/N ratio was computed as the molar ratio between TOC and TN.

2.3.2 Grain size analysis

Grain size analysis was carried out in the Environmental Radioactivity & Sedimentology Laboratory (IONTU) using a Beckman Coulter LS13 320 Laser Diffraction Particle Analyzer with a measurement range of 0.375–2000 µm. All samples were pretreated following the protocol of Poppe et al (2000). Briefly, carbonates were removed using 10% hydrochloric acid (HCl). Carbonate-free samples were then treated with 15% hydrogen peroxide (H_2O_2) for 1 to 2 days to remove organic matter. Ultrasonic devices and sodium hexametaphosphate ($Na(PO_3)_6$) were used to de-flocculate and disperse sediment grains prior to grain size analysis. Relative abundances (reported in percentage) of clay (<4 µm), silt (4–63 µm) and sand (>63 µm) were calculated from the grain size data of bulk sediment.

2.4 Data treatment and statistical analyses of environmental data

Water temperature, salinity, fluorescence, and dissolved oxygen data collected during the last 11.5 years (March 2004 to September 2015) were requested from Ocean Data Bank (ODB) of the Ministry of Science and Technology – Republic of China (2022) to examine environmental control on the spatial distribution of foraminiferal abundance and its associated indicators.

To improve the spatial representativeness of spatially sparse and inhomogeneous hydrographic data, the ODB data set was first gridded and then each sediment site was matched to the closest ODB data grid for the extraction of the hydrographic data. The hydrographic data were then averaged to obtain the mean annual value for each parameter. Sparse temporal sampling of this dataset does not allow a meaningful calculation of monthly average.

The hydrographic parameters were grouped into surface and bottom conditions. Surface condition was defined as 0–400 m water depth. We selected this water depth range because most of the planktic foraminifera species live within this range (Schiebel and Hemleben 2017 and references therein). Meanwhile, bottom condition corresponds to the hydrographic data closest to the seafloor as an approximation of the bottom water conditions influencing benthic foraminifera that live on/in the sediment. Specifically, we used the average values of the last 10 m, 50 m, 100 m, and 500 m of the water column for stations located in <100 m, 100–500 m, 500–1000 m and 1000–2500 water depth, respectively. In the case of stations located below 2500 m water depth we averaged the data from 2500–3500 m of the water column. Statistical analyses including correlation coefficients were performed using statistical software PAST 4.09 (PAleontological STatistics) (Hammer et al., 2001).

2.5 Regression analysis and reconstruction uncertainty

The relationship between %P and water depth follows an exponential function. For ease of analysis, we log-transformed the exponential equation, and reported the regression lines as ordinary least squares linear regression, as follows:

Exponential function: Water depth = a*exp(b*%P)

After log-transformation: log(water depth) = log(a) + b*%P

; where regression slope = b, and intercept = log(a).

To obtain robust regression fits for regional and global data sets such as those reported in Figs. 4 and 10, we adopted a "remove and refit" approach. That is, we first fitted an initial regression line to the data sets. Data points falling outside of the 95% prediction bounds (2σ) are considered outliers. These "anomalous" or "biased" data were then removed from the data set before the final regression line was refitted. Thus, all the reported regression lines only consider data points within the 95% prediction bounds (2σ) of the initial regression model. The uncertainty (2σ) associated with the paleobathymetric estimates derived from these regression lines (Fig. 10d) was obtained by propagating the standard error of the slope and intercept through the calculation. We note that our global compilation does not contain datasets from subarctic waters where the planktic foraminifera are generally smaller in size, thus higher %P values may be obtained when a smaller size fraction is used. However, due to the data volume of our compilation, future inclusion of subarctic datasets is unlikely to significantly affect the global regression.

3. Results

3.1 Correlation between foraminifera and environmental parameters

Correlation coefficients between foraminiferal indices (%P, planktic, and benthic foraminiferal abundance) and environmental parameters, including bulk sediment data (%Sand and TOC content) and hydrographic data (temperature, salinity, fluorescence, dissolved oxygen), are presented in Table 1. The correlations between planktic foraminiferal and environmental parameters of the upper water column (0–400 m) are relatively weak ($R < 0.36$), with the strongest correlation observed for fluorescence and water depth. Of all parameters, benthic foraminiferal abundance shows the strongest correlation with water depth ($R = -0.65$), and weaker but statistically significant correlations with parameters related to food availability i.e., fluorescence ($R = 0.25$), TOC ($R = -0.39$) and bottom water oxygen content ($R = 0.42$). %P derived from the ratio of planktic and benthic foraminiferal abundances, on the other hand, shows in general stronger relationships with environmental parameters. Of all the variables, the

strongest correlation is found between water depth and %P (R = 0.57). %P is more strongly correlated to planktic foraminiferal abundance (R = 0.76) than to benthic foraminiferal abundance (R = -0.48). Parameters associated with ocean productivity show relatively weak correlations with %P and in opposite directions; fluorescence and bottom water dissolved oxygen correlate negatively with %P (R = -0.49 for fluorescence and R = -0.35 for bottom water dissolved oxygen) while the TOC correlates positively with %P (R = 0.26) (Table 1).

>>Table 1<<

3.2 Abundance of benthic foraminifera in surface sediments off Taiwan

The abundance of benthic foraminifera (>125 μm) at sites off Taiwan ranges from 0 to 169 ind. g^{-1} (Fig. 2c), with a median value of ~5 ind. g^{-1} (orchid boxplot in Fig 2a). The median abundance of benthic foraminifera varies by region, ranging from ~1 to ~10 (Fig. 2a). The highest abundance is observed in the Changyun Sand Ridge (~10 ind. g^{-1}), while the lowest abundances occur in Taitung-Hualien (~3 ind. g^{-1}) and Hoping-Nanao-Hateruma Basins (~1 ind. g^{-1}). Meanwhile, intermediate abundances are observed in the Gaoping (~7 ind. g^{-1}), Southern Okinawa Trough (~6 ind. g^{-1}), and Hengchun Ridge (~6 ind. g^{-1}).

When considered by site, the spatial distribution of benthic foraminifera (Fig. 2e) is characterized by high abundance off Changyun Sand Ridge, Gaoping, Hengchun Ridge and several Southern Okinawa Trough sites near the Ryukyu Arc. Notably, the highest abundance of benthic foraminifera of the entire data set occurs in the Southern Okinawa Trough (169 ind. g^{-1}) (Fig. 2e). Most samples from the Hoping-Nanao-Hateruma Basins and Taitung-Hualien contain relatively low abundance of benthic foraminifera (Fig. 2a and 2e). Benthic foraminiferal abundance broadly decreases with increasing water depth (Fig. 2c), with some spatial variability within the Gaoping and Southern Okinawa Trough (Fig. 2c and 2e). In the Gaoping sector, samples from Gaoping Submarine Canyon show relatively low benthic foraminiferal abundance compared to samples from a similar bathymetric range off Southwestern Taiwan (Fig. 2c and

S1). Meanwhile, samples from the Southern Okinawa Trough show a large range of benthic foraminiferal abundance for a narrow range of bathymetry between 1500–2000 m (Fig. 2c).

>> Figure 2 <<

3.3 Abundance of planktic foraminifera in surface sediments off Taiwan

The planktic foraminiferal abundances (>125 μm) off Taiwan range from 0 to ~1000 ind. g^{-1} (Fig. 2d), with a median value of ~14 ind. g^{-1} (orchid boxplot in Fig 2b). The planktic foraminiferal abundance varies substantially by region, with extremely low to no presence in the Changyun Sand Ridge. The highest abundance occurs in the Fengchun Ridge sector (~155 ind. g^{-1}), while intermediate to low abundances occur in the Taitung-Hualien (~27 ind. g^{-1}), Hoping-Nanao-Hateruma Basins (~23 ind. g^{-1}), Gaoping (~15 ind. g^{-1}) and Southern Okinawa Trough (~11 ind. g^{-1}) sectors (Fig. 2b).

When considered by site, the spatial distribution of planktic foraminifera shows an increase in abundance with increasing water depth (Fig. 2d and 2f), more obvious off West Taiwan (e.g., Gaoping sector) than off East Taiwan. There is substantial scatter in the data from Gaoping sector as planktic foraminiferal abundances are anomalously low in the sediments of submarine canyons compared to the rest of the Gaoping data set, thereby forming two separate clusters in the scatter plot (Fig. 2d). The Southern Okinawa Trough and Hoping-Nanao-Hateruma Basins data show a large spread in planktic foraminiferal abundances within a small bathymetric range (Fig. 2d). Interestingly, the planktic foraminiferal abundance in Hoping-Nanao-Hateruma Basins appears to decrease sharply with water depth (R^2 = 0.8; exponential fit), in the opposite direction of the overall regional relationship between planktic foraminiferal abundance and bathymetry. Due to the larger scatter in the dataset (Fig. 2d), the overall correlation between water depth and planktic foraminiferal abundance is weaker than that for benthic foraminiferal abundance (Table 1).

>> Figure 3 <<

3.4 Planktic foraminiferal percentage (%P) off Taiwan

Out of 119 samples, only 88 (67) samples yield >50 (>100) individuals of benthic and planktic foraminifera (Fig. 3a). Both sets of data (>50 and >100) yield comparable regressions with similarly good fit (Fig. 3a; method in Section 2.5; discussion in Section 4.2). In the following, we consider only samples containing >50 counts for our results and discussion of %P (Section 2.2). Fig. 3 shows the spatial distribution of %P off Taiwan, which is in the range of 0 and 99.8 % (Fig. 3b and 4a). In general, as expected the %P value in the sediments off Taiwan increases with increasing water depth (R^2 = 0.72; exponential model) (Fig. 4a). %P values in the Changyun Sand Ridge and Hengchun Ridge sectors off West Taiwan generally follow the regional trend of %P and water depth (Fig. 4a). Compared to these sectors, larger scatter and variability (within a bathymetric range) can be observed in the Southern Okinawa Trough and Gaoping sectors, even though on average %P values in these sectors do increase with increasing water depth (Fig. 4a). The scatter in these datasets is evident as data points that lie outside the 95% prediction bounds of the regression are mostly from these two sectors in addition to one site from Hoping-Nanao-Hateruma Basins (Fig. 4a). Data dispersion in these sectors is further depicted using boxplots grouped by depth-bin (Fig. 4b). Interestingly, the largest data dispersion in each sector seems to be associated with a particular bathymetric range, i.e., 0–500 m depth for Gaoping sector, 1000–1500 m depth for Southern Okinawa Trough region and 3000–4000 m depth for Hoping-Nanao-Hateruma Basins (Fig. 4b). Water depth estimates derived from the regression equation (after outlier removal) are mostly within ~1000 m of the actual water depth at the site, except for those in the deep Hoping-Nanao-Hateruma Basins which are associated with larger errors (1000–2500 m) (Fig. 4c). The residuals are generally smaller at shallow water depth <200 m and increase with water depth.

>> Figure 4 <<

3.5 Grain size and bulk geochemistry

In our sediment collection, silt is the dominant size class with a mean contribution of ~65% (Fig 5a). The clay and sand size classes are less abundant with a mean value of 17% and 18%, respectively. The spatial distribution of sand/silt/clay size classes differs between the designated regions of East and West Taiwan (Fig. 5b and 5c). Fine-grained size classes (i.e., clay and silt) dominate the regions in East Taiwan (Fig. 5b), while West Taiwan is marked by a larger presence of coarser sand fraction (Fig. 5c). Overall, the sand content decreases with increasing water depth. In West Taiwan, the "sandy" sediments are mostly restricted to the Changyun Sand Ridge (<50 m; see Fig. 1) and mostly the shelf (<200 m) of the Gaoping sector or close to the mouth of the Gaoping River, while in East Taiwan coarser sediments are restricted to the area influenced by the Lanyang River in the Southern Okinawa Trough (Fig. 5b and S1). In the deep Hoping-Nanao-Hateruma Basins, the surface sediments are mainly composed of silt and clay, but the sand content can be as high as 7% at a few sites (Fig. 5b).

The TOC content and C/N ratios are relatively low in most sediments off Taiwan (Fig. 5d-g), with median values of 0.7 wt% and ~8 respectively (Fig. 5d and 5e). Samples from the Changyun Sand Ridge contain the lowest TOC content. The lowest C/N ratios are found in the Gaoping sector, while the highest TOC content and C/N ratio were observed in the Southern Okinawa Trough (Fig. 5d and 5e). The overall low C/N ratios in the surface sediments (<10) indicate that the organic matter in these sediments is predominantly marine in origin. The exception to this trend is two stations in the Southern Okinawa Trough with TOC content and C/N values >1.9 wt% and >15, respectively, substantially higher than the rest of the dataset (Fig. 5d,e and Fig S5). Both TOC content and C/N ratio show statistically significant correlation ($p < 0.05$) with water depth (Fig. 5d and e), with $R^2 = 0.38$ for C/N ratio and $R^2 = 0.69$ for TOC.

>> Figure 5 <<

4. Discussion

4.1 Assessing potential bias on %P value due to low foraminiferal counts and size fraction choice

There is no consensus on which size fraction to use for %P analysis. For instance, half of the regional data sets we compiled used the >63 µm fraction while the other half used the larger >125 µm fraction. The choice of size fraction may have an impact on the total foraminiferal counts due to the fact that the abundance of small juvenile specimens (i.e., <125 µm) can be several times larger than the number of bigger adult specimens (i.e., >125 µm). This could potentially lead to different %P results depending on the size fraction selection, i.e., >125 µm vs. >63 µm. In order to assess this potential caveat, we compared a subset (n = 30) of samples covering a large range of water depths (~20–~3600 m), %P (0–99%), and sedimentation conditions (i.e., stations falling within ("normal") and outside ("anomalous") the 95% prediction bounds (2σ) of the regression fit (see section 2.5)).

Overall, our analysis shows that the choice of size selection has no bearing on the %P results (Fig. 6). The abundance of benthic foraminifera in both size fractions i.e., >63 µm and >125 µm, share the same primary relationship with water depth (Fig. 6a), despite higher counts in >63 µm as expected. %P values calculated from the >63 µm size fraction show a strong correlation with the %P values calculated from the >125 µm size fraction (Fig 6b), with a mean difference of only 3.5% in the %P value without any systematic offset. The regressions based on these data sets are also comparable (Fig. 6c) and the slope of the regressions agree within error (>63 µm slope = 0.0442 ± 0.0052 vs. >125 µm slope = 0.0418 ± 0.0047). Interestingly, the scatter in the >63 µm data set is slightly larger than that in the >125 µm data set, as indicated by its lower R^2 value (Fig 6c). Altogether, these findings suggest that size fraction selection (>125 µm vs. >63 µm) has little effect on the regression between %P and water depth. In summary, our results reinforce previous suggestion that the use of the size fraction >63 µm or >125 µm in the calculation of %P led to similar conclusions (Hayward et al., 2019).

To the best of our knowledge, there is no consensus in the literature concerning the minimum foraminiferal tests (counts) needed for a robust interpretation of %P. Most studies

advocate the use of at least 100 tests for the census count, up to as high as 500 (Gibson, 1989; Nigam and Henriques, 1992; Schmuker, 2000; van der Zwaan et al., 1990; van Hinsbergen et al., 2005; van Marle et al., 1987). In this study, due in part to the small sample size, it was not always possible to reach 100 tests per sample for census count. We note that Hayward et al (2019) recently demonstrated that census counts based on >50 tests yield robust results for %P distribution in sediments off New Zealand. To evaluate if this is also true for our %P dataset, we compared data based on >50 and >100 counts (Fig. 3a). We do not observe any systematic offset between these two datasets. Furthermore, the regression lines based on data with >50 counts and >100 counts show a similar relationship with comparable R^2 values (R^2 of >50 counts = 0.72, R^2 of >100 counts = 0.70), suggesting that including %P data based on >50 counts in our Taiwan dataset does not bias the %P values nor the relationship between %P and water depth. Therefore, the threshold of 200 to 400 counts normally recommended for foraminiferal assemblage studies (Schönfeld et al., 2012) may not be necessary for %P analysis. To assess this possibility, we examined the >63 µm (containing more specimens; see discussion in the previous paragraph) fraction from a subset of our samples (n = 30). The data show that the use of different count thresholds i.e., total counts ≥50, ≥200, and ≥400, has little effect on the %P-water depth relationship as all the regression lines agree within error (95% prediction bounds; Fig. S2). In fact, the 50 counts data set performs better (highest R^2 value) than others as it contains more data points and covers a larger range of water depth and %P value. This implies that whilst a higher count threshold may yield stronger statistical representativeness of the %P value, the resultant smaller data set leads to a less reliable regression model. These findings are in agreement with the results from New Zealand (Hayward et al., 2019). Hayward et al. (2019) pointed out that the interpretation of samples with counts <50 specimens is not necessarily invalidated if all the tests in the size fraction are being considered, but the uncertainty of the interpretation will be higher.

>> Figure 6 <<

4.2 Environmental controls on foraminiferal abundance and %P

Previous studies have suggested that %P in marine sediments may be influenced by regional hydrography, such as the spatial extension of the monsoonal upwelling (van Marle et al., 1987) and land-sea salinity gradients (Nigam and Henriques, 1992). To assess the influence of hydrographic variables on foraminiferal abundance off Taiwan, we examine the correlation between foraminiferal indices (foraminiferal abundance and %P) and hydrographic data (surface and bottom) as well as bathymetry (Table 1). Our results show that %P has the strongest correlation with water depth (bathymetry) among all environmental variables, as expected, suggesting that off Taiwan the water depth of depositional setting exerts the strongest control on %P, hinting at its potential as a proxy for paleobathymetric reconstruction.

Ocean productivity (i.e., fluorescence and TOC) and bottom water oxygen content are considered relevant drivers of foraminiferal ecology (Gooday, 2003; Schiebel and Hemleben, 2017). In the case of planktic foraminifera, high ocean productivity generally leads to high foraminiferal abundance due to high food availability (Schiebel and Hemleben, 2017; Tapia et al., 2022). Planktic foraminiferal abundance may coincide with the peak of fluorescence at a certain depth in the water column. Curiously, we do not observe any strong correlation between planktic foraminiferal abundance and productivity parameters such as sedimentary TOC and seawater fluorescence. This might have to do with the substantial scatter in the planktic foraminiferal abundance data. Another reason might be due to the inherent flaw of the approach in correlating the average fluorescence of the upper 0–400 m water column with foraminifera data, whereas the abundance of foraminifera likely follows the peak fluorescence at a certain depth that varies from site to site.

In the case of benthic foraminifera, the effect of ocean productivity (i.e., TOC) and bottom water oxygen content are highly complex and not always straightforward (Jorissen et al., 2007, 1995). Generally speaking, as surface ocean productivity increases, the flux of organic matter (food) to the seafloor tends to increase as well. Higher fluxes of organic matter to the seafloor may help benthic foraminifera to thrive; however, the decomposition of a large amount of organic matter may lead to a depletion of the bottom water oxygen content due to the higher oxygen

demand by more active remineralization. One effect of the oxygen depletion on benthic foraminifera is a shift in the size distribution toward the smaller size class (i.e., 63–125 μm) (Bernhard and Sen Gupta, 1999; Sen Gupta and Machain-Castillo, 1993), a condition that may affect our %P data as they are based on the foraminiferal abundances >125 μm. However, as discussed above, we do not observe any discernible difference in the %P results between the >63 μm and >125 μm fractions (Fig. 6). Further, we posit that oxygen content is an unlikely driver of %P off Taiwan as the lowest oxygen value of the bottom water (~54.3 $\mu molL^{-1}$) in the study area is almost three times as high as the threshold (22 μmL^{-1}) that is known to affect foraminiferal dynamics (Levin and Gage, 1998). The ecological response of benthic foraminifera to environmental parameters is highly complex, however our data show that bathymetry exert the strongest control on benthic foraminifera. This finding is in agreement with the concept that food (quantity and quality), the most relevant controlling factors of benthic foraminiferal ecology (Beck Eichler and Barker, 2020; Gooday, 2003; Jorissen et al., 2007, 1995; van der Zwaan et al., 1999) is somehow modulated by water depth. Overall, our data show that bathymetry still exerts the strongest control on the spatial distribution of %P despite minor influences from other hydrographic parameters.

4.3 %P-water depth relationship in different geological and sedimentological settings off Taiwan

In general, the %P value off Taiwan increases exponentially with water depth ($R^2 = 0.72$; Fig. 4a). Notably, some data from the Southern Okinawa Trough, Hoping-Nanao-Hateruma Basins, and the Gaoping sector deviate strongly from the general trend (Fig. 4).

The distribution of foraminiferal tests in the sediments is modulated by the interplay of the (1) production of foraminiferal test and sedimentation rate; (2) transport of foraminiferal test by ocean currents (3) destruction (dissolution) (4) reworking of sediment and subsequent downslope transport and redeposition (Schmuker, 2000). Consequently, any index based on foraminiferal material will be susceptible to the above-mentioned processes. Indeed, previous studies have attributed the occurrence of “anomalously” low or high %P values to downslope

sediment transport (Hayward et al., 2019), or calcite dissolution in organic-rich sediments (in front of Mississippi River, Gulf of Mexico) (Parker, 1954). In the following three sub-sections, we discuss possible factors causing the anomalously low %P values in the Southern Okinawa Trough sector (section 4.3.1), Hoping-Nanao-Hateruma Basins (section 4.3.2), and submarine canyons in the Gaoping sector (section 4.3.3).

4.3.1 Low planktic foraminiferal abundance and downslope sediment transport in Southern Okinawa Trough

Overall, the %P distribution in the Southern Okinawa Trough is characterized by relatively low values (Fig. 3b and 3c) and substantial variability, especially in the bathymetric range of ~1000–1500 m (Fig. 4c). Here, despite a moderate abundance of benthic foraminifera, the planktic foraminiferal abundance is the lowest among all the sectors assessed (Fig. 2a and 2b). Despite the lower-than-average planktic foraminiferal abundance, it is still twice as large as that of benthic foraminiferal abundance (compare the median values of gray boxplot in Fig. 2a and 2b). Therefore, the variability in %P here is likely driven by the variability in planktic foraminiferal abundance.

The abundance of planktic foraminiferal tests in sediments reflects the balance between the destruction and preservation of these calcite tests. Consequently, a low number of foraminiferal tests in surface sediments in the Southern Okinawa Trough might be the result of conditions that favor the destruction of the foraminiferal calcite tests. The preservation of carbonate in sediments varies as a function of the solubility of the carbonate in the seawater, with high (low) solubility favoring the destruction (preservation) of the foraminiferal calcite (Berger and Diester-Haass, 1988; Bostock et al., 2011). The depth where the solubility of the calcite changes is known as Calcite Saturation Horizon (CSH) (Bostock et al., 2011), and its position in the water column varies across basins as a function of the water pressure, in-situ temperature, and water chemistry. The modern Calcite Saturation Horizon in the Southern Okinawa Trough is located at ~1600 m water depth (Fig. 7a; transect P03-W, GLODAPv2 dataset, Olsen et al., 2019), close to the lower end of the bathymetric range characterized by large %P variability.

Therefore, it is possible that the low number of foraminiferal tests in this sector reflects a relatively shallow position of the CSH causing calcite dissolution. However, the abundance of planktic foraminifera below (1600 – 1800 m) and above (1400 – 1600 m) the CSH show no significant change (Fig. 7a), arguing against calcite dissolution as the main driver of the low presence of planktic foraminiferal tests in the sediment.

The production of planktic foraminiferal tests in the water column is generally related to water fertility (Schiebel and Hemleben, 2017; Tapia et al., 2022). Consequently, the oligotrophic Kuroshio Current flowing northward along the eastern coast of Taiwan (Liang et al., 2003) may reduce the planktic foraminiferal abundances and, in turn, the %P in the Southern Okinawa Trough. However, relatively high planktic foraminiferal abundances and %P values occur at some sites within the Southern Okinawa Trough (Fig. 7c) and at sites located offshore the eastern flank off Taiwan along the path of Kuroshio Current (i.e., Taitung-Hualien and Hoping-Nanao-Hateruma Basins) (Fig. 3b). Moreover, the Southern Okinawa Trough is influenced by topographically steered upwelling centers that further fertilize the upper ocean, increasing its fertility (Jan et al., 2011; Lee et al., 2004). Altogether these findings suggest that lower ocean fertility due to Kuroshio Current is not the main driver of the low and variable %P values in this basin.

>> Figure 7 <<

The amount of exported carbon to the seafloor generally reflects the marine productivity in the euphotic zone. Therefore, the organic carbon content in surface sediments may shed light on the relationship between marine productivity and %P. Interestingly, the TOC content in the sediments from the Southern Okinawa Trough is slightly higher than the rest of the dataset. If the aforementioned positive relationship between marine productivity and %P applies to this region, high TOC content in the Southern Okinawa Trough argues against low water fertility as the main reason for the low planktic foraminiferal content in the sediments. In the Southern Okinawa Trough (Fig. 5d), the TOC content further away from land (>1000 m water depth) is higher than

the TOC content on the adjacent shelf and the mouth of the Lanyang River (Fig. 5f, g). Kao et al. (2003) attributed this pattern to the overprint of the riverine export, as the low TOC values near the river mouth reflect a strong mineral dilution effect, a distinctive characteristic of mountainous watersheds off Taiwan (Jeng et al., 2003; Kao and Liu, 1996; Kao et al., 2003). Meanwhile, the higher TOC content in the Southern Okinawa Trough may be a consequence of the seaward extension of the fine-grained sediment belt from the inner shelf of the East China Sea (Kao et al., 2003).

The topographic constraint of the Kuroshio Current against the East China Sea leads to a southwest flow and the formation of 100 km cyclonic eddies centered on the Mien-Hua Canyon (Chen et al., 2017; Chiang et al., 2022; Chung et al., 2003; Kao et al., 2003; Lee et al., 2004). These eddies promote the retention and resuspension of suspended particles on the slope of the East China Sea shelf. Sediment trap observations have shown that the total particulate matter fluxes are particularly high within the Mien-Hua canyon, with mean mass fluxes ranging from 6.64 to 71.5 g m-2 day-1, substantially higher than nearby slope areas (0.77–15.7 g m-2 day-1) (Hung et al. 1999). From here, the sediments are transported downslope by gravity flows to the deeper parts of the Southern Okinawa Trough (Chen et al., 2017; Chiang et al., 2022; Chung et al., 2003; Kao et al., 2003; Lee et al., 2004).

Indeed, previous studies in the Southern Okinawa Trough concluded based on sedimentary ^{210}Pb data that in addition to hemipelagic sedimentation, gravity flows (i.e., turbidity flow) are the main source of sedimentary material here sedimentary transport processes (Huh et al., 2006, 2004). Huh et al. (2006) noted that 1) the sites located on the slope had a lower ^{210}Pb mass accumulation rates relative to sites at the same water depths further offshore Taiwan and 2) that a depression at the base of the slope below the 1400 m isobath in the western part of the Southern Okinawa Trough between 122.3 and 122.7 ºE was characterized by extremely high sedimentation rates (0.4 – ~1.5 cm yr^{-1}). The authors interpreted this pattern as the result of the transport of sedimentary material from the slope toward the basin floors via episodic inputs of turbidites triggered by earthquakes, which then led to the formation of a zone of ~300 km^2 of “abnormally” high sediment input (Huh et al., 2006, 2004; Lee et al., 2004). Interestingly, the

lowest %P values observed in the Southern Okinawa Trough (Fig. 8a) occur within this zone. The grid 25–24.75 ºN and 122.3–122.7 ºE is characterized by sedimentation rates >1 cm y^{-1} (Fig. 8a). The sites in this grid cover a relatively small bathymetric range between ~1000 – ~1500 m water depth, but %P values vary substantially between 25% to 80% (Fig. 4b). Given the bathymetric range, the expected %P values as observed in other regions should be in the range of 85% and 94%, but values as low as 25% that is typical for shallow shelf can be observed in the Southern Okinawa Trough (Fig. 4a). In line with previous studies, gravity flows triggered by earthquakes may be a mechanism via which sediments from the shelf and slope can be transported to the deeper part of the basin. As sediments from the shelf typically contain low planktic foraminiferal content and low %P value, the presence of these sediments in the deep basin would thus lead to lower values in %P and planktic foraminiferal abundance, as observed in the Southern Okinawa Trough. The occurrence of gravitationally displaced individuals e.g., shallow water genera such as *Amphistegina*, *Calcarina*, *Neorotalia*, *Elphidium* (Fig. S2) in the surface sediments of some stations located below ~1000 m water depth (stations OR1-642-BC22; OR1-0715-20; see Fig. S5 for site location) also argue in favor of the supply of sediments from shallower depths via gravity flows. Taken together, we argue that the low concentration of planktic foraminifera in the Southern Okinawa Trough surface sediments (Fig. 2b) may have been a result of the dilution of the locally produced biogenic material by detrital material transported by gravity flows.

>> Figure 8 <<

4.3.2 Possible bias by carbonate dissolution on %P values in the Hoping-Nanao-Hateruma Basins

The %P values of sediments from the Hoping-Nanao-Hateruma Basins are amongst the highest off Taiwan (Fig. 4a), despite the relatively low planktic foraminiferal abundance here compared to other pelagic regions with bathymetry >2000 m such as Hengchun Ridge (Fig. 2b). Nevertheless, the planktic foraminiferal abundance in these basins are >20 times higher than the

benthic foraminiferal abundance (see sections 3.2 and 3.3; Fig. 2), thus exerts a stronger influence on the %P values than does its benthic counterpart. Notably, in contrast to the general positive relationship with bathymetry (Fig. 2d), planktic foraminiferal abundance in the Hoping-Nanao-Hateruma Basins decreases with increasing water depth (Fig. 7b), with the largest variability occurring within the Carbonate Saturation Horizon located at ~3000 m. The aforementioned relationship between planktic foraminiferal abundance and water depth plus the fact that the average water depth in this region is ~3500 m both indicate that carbonate dissolution maybe an issue here.

The %P values in the Hoping-Nanao-Hateruma Basins are within a small range between ~86 and 99.8 % except for the site MD18-3531BC (water depth of 3590 m; location marked in Fig. S5) where the %P value = ~51%; (Fig. 4a). We do not have %P value for deeper sites because the foraminiferal counts here do not pass the threshold of at least 50 counts. Site MD18-3531BC is characterized by a planktic foraminiferal abundance (3.7 ind. g^{-1}) (see Table S1) several times below the average of this region (~23 ind. g^{-1}; Fig. 2a). The site is located below the Carbonate Saturation Horizon where carbonate dissolution is extensive. The tests of planktic foraminifera are more susceptible to dissolution than those of benthic foraminifera (Corliss and Honjo, 1981; Regenberg et al., 2013), thus it is plausible that the low %P value (~51%; Fig. 4a) at site MD18-3531BC reflects the preferential loss of planktic foraminiferal tests due to carbonate dissolution. Interestingly, the %P values at the other two sites in the Hateruma Basin (MD18-3529BC and MD 18-3530BC; %P >89) are much higher than that at MD18-3531BC (Fig. 9, locations marked in Fig S5). These sites are ~100–200 m shallower than site MD18-3531BC but still below the Carbonate Saturation Horizon, thus should be equally susceptible to carbonate dissolution. The sites in the Hateruma Basin are also marked by large variability in planktic foraminiferal abundance, ranging from 3.7 ind. g^{-1} to 72 ind. g^{-1} (Fig. 9). Given the proximity of the sites (see Fig. 1 and Fig. S5) and thus similarity in hydrography, it seems unlikely that this variability stems from large changes in the fluxes of planktic foraminifera or vastly different sedimentation rates.

In a recent study based on several downcore profiles in the eastern part of the Hateruma Basin, Ikehara et al. (2022) observed the occurrence of coarse calcareous sand layers (calciturbidite) at 7–8 cm below seafloor and attributed it to seismic activity (tsunami), which triggered the transport of sedimentary material formed in the corals reefs of the southern Ryukyu islands (i.e., Hateruma, Iriomote and Ishigaki islands) toward the deeper part of the Hateruma Basin. Meanwhile, mineralogical data of the surface sediment at site MD18-3531BC indicate that the clay minerals here originate from the Ryukyu arc massif and islands located next to the Hateruma Basin (Nayak et al., 2021). Taken together, it is plausible that our surface sediments recovered from the Hateruma Basin may also have been influenced to some degree by downslope transport of sediments. We hypothesize that the variability in planktic foraminiferal numbers in the rather small Hateruma Basin may reflect downslope transport of sediment from relatively deep localities (>1000 m) where the %P value is similar to that in the autochthonous sediments. This scenario is partially supported by the grain size distribution in the Hoping-Nanao-Hateruma Basins. Here, several studies have used grain size changes to identify turbidites from sediment of hemipelagic origin (Dezileau et al., 2016; Lehu et al., 2015; Nayak et al., 2021). Turbidites typically appear as departures from fine sediments (hemipelagic <10 µm) (Lehu et al., 2015) toward coarser sizes. The surface sediment of the core MD18-3531BC show the highest percentage of sand (>63 µm) among the sites in the Hateruma Basin (Fig. 9), suggesting a possible turbidite origin of the sediment. Our results show that the complex interplay between carbonate dissolution and downslope transport that is highly variable in space (Lehu et al., 2015; Nayak et al., 2021; Ikehara et al., 2022) alters the relationship between %P and bathymetry in the sites in Hoping-Nanao-Hateruma Basins (e.g., quick isolation of foraminifera tests by event deposits may improve the calcite preservation). Allochthonous sediments, especially those from a much shallower depth may alter the proportion of planktic and benthic foraminiferal tests in the sediments, while dissolution preferentially removes planktic foraminiferal tests from the sediment; both scenarios lead to lower %P values. A qualitative estimation of the dominant factor on the %P (depth v. dissolution v. downslope transport) might

be possible by considering additional information such as grain size distribution, total abundances of planktic foraminifera, fragmentation, and foraminifera fauna.

>> Figure 9 <<

4.3.3 Low foraminiferal abundance and %P values in submarine canyons off Southwestern Taiwan

The sediments located in submarine canyons (Gaoping and Fangliao; see Fig. 1d) are characterized by particularly low abundances of planktic and benthic foraminifera, compared to other samples collected from the Gaoping sector (Fig. S4). As this low abundance only occurs within the canyons it is unlikely to be caused by processes involving a large spatial coverage i.e., production and preservation (dissolution). Instead, smaller scale processes associated with the canyon dynamics are more likely to be responsible for the low foraminiferal abundance.

The Gaoping River provides 23 to 45 Mt yr^{-1} of terrestrial material to the Gaoping Submarine Canyon (Huh et al., 2009; Lee et al., 2015). If deposited in the canyon, such a large amount of terrestrial material may in principle dilute the biogenic component of marine origin in the sediment. Riverine runoff is heavily influenced by regional climatic patterns. For instance, typhoons can exert a strong effect on the delivery of material to the canyon as the heavy rains on the upstream catchment area increase the flow rate of the Gaoping River as well as its sediment load (Lee et al., 2015; Liu et al., 2009, 2006). As a typhoon approaches, events of sediment-flushing down-canyon (as gravity flow) occurs (Chung et al., 2009; Huh et al., 2009; Lee et al., 2009b, 2009a; Liu et al., 2009, 2006; Su et al., 2012). Su et al (2012) highlighted the high energy associated with these gravity flows events as they were the most likely culprit of the submarine cable breakage at the landfall of the typhoon Morakot between 7 to 9 of August (2009). Due to this process, only 20% of the riverine sediment load from Gaoping River is retained in the canyon, the rest of it being delivered to the deep basin (Huh et al., 2009). The constant flushing of sediment also leads to relatively low sedimentation rates in the canyon relative to the neighboring shelf (Hu et al., 2009; Fig 8b). Therefore, it is plausible that gravity flows may

remove foraminiferal tests along with the rest of the sediments from the uppermost parts of the canyon and transport them downslope. As the kinetic energy of the gravity flow dissipates some foraminiferal test may be released and re-deposited at different parts of the canyon. These processes might lead to low foraminiferal abundance in the canyons.

Typhoons also result in cross-shelf transport. For instance, benthic foraminifera have been found in a set of sediment traps moored off the Gaoping River during the landfall of the typhoon Kay-tak (2000) (Lin et al., 2005). The isotopic compositions of the benthic foraminifera recovered from the upper (186 m) and lower (236 m) traps suggest calcification depth <50 m, thus they must have been transported from shallower localities (Lin et al., 2005). This finding highlights a connection between typhoon occurrence and cross-shelf transport of foraminiferal tests, which may transport low %P sediments (due to higher abundance of benthic foraminifera) from the shallow shelf to the deep canyon and the mixing of sediments will thus lower the %P value in the canyon. Foraminiferal abundance at most sites in the Gaoping and Fangliao submarine canyons is too low for %P calculation. The only three canyon sites containing enough foraminiferal tests (n>50) for the %P calculation, namely OR3-1367-G4 (436 m), OR3-1963-C59 (677 m) (Gaoping Submarine Canyon), and OR1-1188-FL1 (570 m) (Fangliao Canyon), show low %P values for the bathymetric range (Fig. 3d, 4a, S4c and S5) albeit still within the 95% prediction range (Fig. 4a). These low %P values might be a result of the aforementioned cross-shelf transport. It is possible that this type of transport may in part lead to the relatively large scatter in foraminiferal abundance and %P value in the Gaoping sector (Fig. 4a).

On the other hand, high %P (60-95%) values are observed for four sites on the shallow shelf off Southwestern Taiwan at the entrance of the Taiwan Strait, namely OR3-1367-C4 (54 m); OR3-1420-C8 (107); OR3-1367-C45 (133 m), and C49 (169 m) (Fig. 3d and S5). Since the intrusion of the Kuroshio Branch Current and South China Sea Current feed the Taiwan Current that flows across the Taiwan Strait (Fig.1b), the high %P values may be caused by the lateral advection of planktic foraminifera produced further south where the water column is deeper and then deposited on the shallow shelf typically characterized by low abundance of planktic foraminifera (Fig. 2b). In fact, laterally transported planktic foraminifera by East Auckland Current

has also been invoked to explain high %P values in the shelf sediments off New Zealand Northland (Hayward et al., 2010).

4.4 Regional and global regression function of %P–water depth

%P values in marine sediments off Taiwan generally vary with bathymetry (section 4.3) but may be strongly influenced by downslope or cross-shelf sediment transport (section 4.3.1, 4.3.2, 4.3.3), lateral transport of planktic foraminifera (section 4.3.3) and carbonate preservation issues (section 4.3.2). Data affected by these processes (i.e. data points lying outside the 95% prediction bound in Fig. 4a) deviate from the general %P–water depth relationship (Fig. 4a). Therefore, these biased data are omitted from the regression analysis to obtain the "true" %P–bathymetry relationship in autochthonous sediments off Taiwan (n = 81; detail in Method section 2.5; Fig. 4a). The exponential regression function after log-transformation is as follows:

Log(water depth) = 0.04245*%P + 3.3127

, with standard errors of 0.00296 for the slope and 0.2322 for the intercept.

Where a value of %P = 100 would result in a depth estimate of 1916 m, whereas %P = 1 would yield 27 m. In other words, when used to reconstruct bathymetry, this equation will not yield any estimate that is >1916 m; for instance, all the water depth estimates for samples in the Hoping-Nanao-Hateruma Basins are too shallow by ~1500 m (Fig. 4b). Despite a strong correlation indicated by the coefficient of determination (R^2= 0.72), it is clear from the residuals that the water depth estimates may be overestimated or underestimated by ~2000 m (Fig. 4b), with a mean (absolute residual) of ~530 m. Due to its exponential relationship, the error associated with paleobathymetry estimate is a function of %P (Fig. 10d). The regression is better constrained at its lower end, yielding more accurate water depth estimates for shallow regions <500 m, e.g. at Changyun Sand Ridge (mean absolute residual = 5 m) and Gaoping sector (mean absolute residual = 434 m). At its higher end i.e., %P of 80 – 95 %, the errors associated with the water depth estimates can range between 800 to ~1800 m (Fig. 4b). Therefore, although this

exponential regression may be useful as a qualitative tool to reconstruct paleobathymetry off Taiwan, care should be exercised when interpreting the water depth estimates obtained as they may not be interpreted quantitatively, especially at the high end of the %P range (Fig 10d).

The visual comparison of several regional %P-depth datasets (Fig 10a) indicates regional differences. The Taiwan regression slope agrees within uncertainty (95% confidence interval; Fig 10b) with those from other regions except Okinawa. This observation is surprising given the geographical proximity of Okinawa and Taiwan. The difference might have to do with the fact that the Okinawa data set contains only 21 data points, thus may not fully capture the regional relationship between %P and water depth. Regional regressions exhibit a range of slopes between 0.02 and 0.05. Of these, the regression slope off Taiwan is of intermediate value (Fig 10b), similar to that from the Gulf of Mexico, Mediterranean Sea and Southeast coast of US. Combining all the regional datasets (i.e., all data > 63 μm) yields a global calibration (total n = 1077; n = 1004 after removing data that fall outside of the 2 standard deviation band; methodological details in Section 2.5) with a R^2 value of 0.87 (Fig 10c) and the equation as follows:

Log(water depth) = 0.04077*%P + 3.3652

; with standard errors of 0.0005 for the slope and 0.0325 for the intercept.

The global regression line is almost identical to the Taiwan regression line (Fig 10c) but with an improved correlation and substantially smaller error (Fig. 10c) as indicated by its higher R^2 value (Fig. 10c) and overall error (Fig. 10d). The improvement is likely due to the much larger data set which spans a larger water depth range and the entire %P range; this attests to the merit of a global calibration that combines all the data sets despite regional variability. We also tested whether the global calibration is mainly dominated by the Taiwan data set by leaving this data set out of the regression analysis. Our results (Fig 10b) show that the inclusion of the Taiwan data set does not exert a strong effect on the slope of the global calibration. When applied to the Taiwan data set to estimate bathymetry, the global calibration yields slightly larger

residuals (mean = 608 m compared to 530 m from the Taiwan calibration) than those obtained from the Taiwan calibration. This suggests that although the %P-depth relationship off Taiwan is similar to the global relationship, a local calibration might perform better in the reconstruction of water depth despite its slightly lower R^2 value and larger error. Therefore, we recommend performing a regional calibration prior to the downcore application of %P. In the absence of a regional calibration, the global calibration reported in this study may be used instead. At %P = 100, this calibration yields a water depth estimate of 1706 m, i.e. the limit of the calibration model. Due to its exponential fit, the reconstruction uncertainty associated with this global calibration is a function of %P (Fig. 10d), which increases from an error of 2 m at %P = 1 to an error of 209 m at %P = 100.

>> Figure 10 <<

4.5 %P as a tool for the reconstruction of paleobathymetry, paleogeohazard and paleoceanography

Despite the aforementioned uncertainties (section 4.4), the Taiwan %P-depth calibration reported here represents the first of its kind for paleobathymetric reconstructions in this region. The application of this modern analog-based calibration might help to generate at least semiquantitative bathymetry estimates, which can be used to reveal the depositional setting of the many outcrops in Taiwan and to shed more light on processes such as the rapid uplift of the central range of Taiwan since the Plio-Pleistocene. The calibration model may be further refined by increasing the sample size, and the integration of diversity indices and stressor species of benthic foraminifera in the %P calculation.

Our results also demonstrate that %P responds to alterations in the sedimentation process (i.e., downslope transport), manifesting as outliers in the %P-water depth relationship. Off Taiwan, in the sectors of Gaoping and Southern Okinawa Trough, the sites with lower than expected %P values can be explained by the downslope transport of sediment, triggered by typhoons or earthquakes. At deep sites located below the Carbonate Saturation Horizon e.g. in

Hoping-Nanao-Hateruma Basins, carbonate dissolution may also lead to low %P values as planktic foraminiferal tests are preferentially dissolved compared to their more robust benthic counterparts (section 4.3.2). For these deep sites, we suggest that additional proxies such as grain size and abundance of foraminiferal tests and diversity indices to be used in tandem to improve the robustness of the %P. The fact that %P traces downslope sediment transport and lateral transport in the water column (section 4.3.2) also means that it has the potential to flag sites and sediment sequences that are unsuitable for paleoceanographic studies that rely on locally produced biogenic material. Therefore, applying %P downcore allows the reconstruction of past occurrences of gravity flow as well as assessing the sedimentary depth horizons that are suitable for paleoceanographic studies, thereby providing clues on possible links between gravity flows and climate variability. The robustness of gravity flow reconstruction can be further enhanced by applying in tandem other proxies in addition to %P, such as sediment grain size, ^{210}Pb, visual characterization of sediment, and foraminiferal assemblage.

5. CONCLUSIONS

The spatial patterns of planktic and benthic foraminifera test in >100 surface sediment samples off Taiwan were determined and compared with hydrographic and bulk sedimentary parameters (grain size distribution and TOC content). These data were used to assess the potential of %P as a tool to detect downslope sediment transport and reconstruct paleobathymetry.

The following are specific conclusions based on the results:

- The abundance of planktic foraminifera increases with water depth while the opposite is true for the abundance of benthic foraminifera.
- Of all the hydrographic and environmental parameters, %P shows the strongest correlation with water depth. %P-water depth relationship in marine sediments off Taiwan shows the same first-order pattern as in other regions and is similar to the global calibration albeit with a higher uncertainty due to a smaller data set.

- The %P-water depth relationship based on counts with >50 and >400 tests are comparable, suggesting that at least for this dataset the threshold of >50 foraminifera count is reasonable.
- Similar %P-water depth relationships were obtained for >63 μm and >125 μm fractions.
- The %P values of surface sediments in Southern Okinawa Trough, Gaoping Submarine Canyon and Hoping-Nanao-Hateruma Basins are relatively low compared to those from a similar bathymetric range.
    - The low %P values in the Southern Okinawa Trough seem to reflect dilution effect due to the arrival of fine material from the East China Shelf area and material transported downslope by gravity flows toward the base of the basin.
    - Low foraminiferal abundances and %P values in Gaoping Submarine Canyon area are likely a result of cross-shelf and downslope sediment transport.
    - In the Hoping-Nanao-Hateruma Basins the %P seems to reflect the interplay between downslope transport of sediment and carbonate dissolution.
- The obtained %P-water depth (water depth (m) = 27.458*exp(0.042454*%P)) may be useful for deducing paleobathymetry in the range of ~30 to 2000 m water depth off Taiwan.
- %P has the potential to capture alterations in the sedimentation process, therefore its application downcore might help to identify both the occurrence of downslope transport and sequences that are suitable for paleoceanographic reconstruction.

6. Author's contribution

RT, SLH, and CCS designed and conceptualized the study. CCS, HLL, KTJ, YPC, JKL, ITL, SLH, NB, GR, and SKH provided surface sediment samples and/or unpublished TOC and grain size data. SCL and RT prepared and analyzed the sediment samples for foraminifera. SCL analyzed TOC and grain size composition as well as requested hydrographic data. MAB provided support for taxonomic identification. Data analysis was performed by SCL and RT.

Initial draft in the form of a MSc thesis excluding data from the EAGER samples was written by SCL with help from SLH. The final manuscript was written by RT and SLH with the contribution from all co-authors who approved its final version.

7. Acknowledgments

This study was funded by Ministry of Science and Technology (MOST) R.O.C. through grants 108-2116-M-002-008, 109-2116-M-002-014, 110-2116-M-002-007, 111-2811-M-002-113. SLH acknowledges grant 107-2611-M-002-021-MY3. We thank the crew and scientists participating in OR1, OR2, OR3, NOR1 and EAGER cruises. Technical support and laboratory assistance from Shen-Ting Hsu (IONTU) are highly appreciated. We are grateful to two anonymous reviewers for their comments and suggestions, which helped improve the final version of the manuscript.

8. Data Availability Statement

Data generated in this study are available in the Supplement and on the Zenodo database (https://doi.org/10.5281/zenodo.7098320).

9. References

Ash-Mor, A., Bookman, R., Kanari, M., Ben-Avraham, Z., Almogi-Labin, A., 2017. Micropaleontological and taphonomic characteristics of mass transport deposits in the northern Gulf of Eilat/Aqaba, Red Sea. Mar. Geol. 391, 36–47. doi:10.1016/j.margeo.2017.07.009

Ash- Mor, A., Almogi- Labin, A., Bouchet, V.M.P., Seuront, L., Guy- Haim, T., Ben- Avraham, Z., Bookman, R., 2021. Going with the flow: Experimental simulation of sediment transport from a foraminifera perspective. Sedimentology. doi:10.1111/sed.12945

Beck Eichler, P.P., Barker, C.P., 2020. Benthic foraminiferal ecology: indicators of environmental impacts. Springer International Publishing, Cham. doi:10.1007/978-3-030-61463-8

Berger, W.H., Diester-Haass, L., 1988. Paleoproductivity: The benthic/planktonic ratio in foraminifera as a productivity index. Mar. Geol. 81, 15–25. doi:10.1016/0025-3227(88)90014-X

Bernhard, J.M., Sen Gupta, B.K., 1999. Foraminifera of oxygen-depleted environments, in: Modern Foraminifera. Springer Netherlands, Dordrecht, pp. 201–216. doi:10.1007/0-306-48104-9_12

Bostock, H.C., Hayward, B.W., Neil, H.L., Currie, K.I., Dunbar, G.B., 2011. Deep-water carbonate concentrations in the southwest Pacific. Deep Sea Research Part I: Oceanographic Research Papers 58, 72–85. doi:10.1016/j.dsr.2010.11.010

Chang, Y.-P., Chen, M.-T., Yokoyama, Y., Matsuzaki, H., Thompson, W.G., Kao, S.-J., Kawahata, H., 2009. Monsoon hydrography and productivity changes in the East China Sea during the past 100,000 years: Okinawa Trough evidence (MD012404). Paleoceanography 24. doi:10.1029/2007PA001577

Chen, C., Lin, H.-L., 2017. Applying Benthic Foraminiferal Assemblage to Evaluate the Coral Reef Condition in Dongsha Atoll lagoon. Zool. Stud. 56, e20. doi:10.6620/ZS.2017.56-20

Chen, C.-T.A., Kandasamy, S., Chang, Y.-P., Bai, Y., He, X., Lu, J.-T., Gao, X., 2017. Geochemical evidence of the indirect pathway of terrestrial particulate material transport to the Okinawa Trough. Quaternary International 441, 51–61. doi:10.1016/j.quaint.2016.08.006

Chen, C.-T.A., Wang, S.-L., Chou, W.-C., Sheu, D.D., 2006. Carbonate chemistry and projected future changes in pH and CaCO3 saturation state of the South China Sea. Mar. Chem. 101, 277–305. doi:10.1016/j.marchem.2006.01.007

Chiang, C.-S., Yu, H.-S., Neda, A., TuZino, T., 2022. The huapinghsu channel/mienhua canyon system as a sediment conduit transporting sediments from offshore north taiwan to the southern okinawa trough. Front. Earth Sci. 9. doi:10.3389/feart.2021.792595

Chien, F.-C., Kuo, H.-C., 2011. On the extreme rainfall of Typhoon Morakot (2009). J. Geophys. Res. 116. doi:10.1029/2010JD015092

Chung, C.-H., You, C.-F., Chu, H.-Y., 2009. Weathering sources in the Gaoping (Kaoping) river catchments, southwestern Taiwan: Insights from major elements, Sr isotopes, and rare earth elements. Journal of Marine Systems 76, 433–443. doi:10.1016/j.jmarsys.2007.09.013

Chung, Y., Chung, K., Chang, H.C., Wang, L.W., Yu, C.M., Hung, G.W., 2003. Variabilities of particulate flux and 210Pb in the southern East China Sea and western South Okinawa Trough. Deep Sea Res. Part II Top. Stud. Oceanogr 50, 1163–1178. doi:10.1016/S0967-0645(03)00016-X

Corliss, B.H., Honjo, S., 1981. Dissolution of Deep-Sea Benthonic Foraminifera. Micropaleontology 27, 356. doi:10.2307/1485191

Dezileau, L., Lehu, R., Lallemand, S., Hsu, S.K., Babonneau, N., Ratzov, G., Lin, A.T., Dominguez, S., 2016. Historical Reconstruction of Submarine Earthquakes Using ^{210}Pb, ^{137}Cs, and ^{241}Am Turbidite Chronology and Radiocarbon Reservoir Age Estimation off East Taiwan. Radiocarbon 58, 25–36. doi:10.1017/RDC.2015.3

De Rijk, S., Troelstra, S.R., Rohling, E.J., 1999. Benthic foraminiferal distribution in the mediterranean sea. Journal of Foraminiferal Research 29, 93–103. doi:10.2113/gsjfr.29.2.93

Gibson, T.G., 1989. Planktonic benthonic foraminiferal ratios: Modern patterns and Tertiary applicability. Mar. Micropaleontol. 15, 29–52. doi:10.1016/0377-8398(89)90003-0

Gooday, A.J., 2003. Benthic foraminifera (Protista) as tools in deep-water palaeoceanography: environmental influences on faunal characteristics. Adv. Mar. Biol. 46, 1–90. doi:10.1016/s0065-2881(03)46002-1

Hammer, Ø., Harper, D., Ryan, P., 2001. PAST: PALEONTOLOGICAL STATISTICS SOFTWARE PACKAGE FOR EDUCATION AND DATA ANALYSIS. Palaeontologia electronica (Online) 4, 9.

Hayward, B.W., Grenfell, H.R., Sabaa, A.T., Neil, H., Buzas, M.A., 2010. Recent New Zealand deep- water benthic foraminifera: taxonomy, ecologic distribution, biogeography, and use in paleoenvironmental assessment.

Hayward, B.W., Sabaa, A.T., Triggs, C.M., 2019. Using foraminiferal test-size distribution and other methods to recognise Quaternary bathyal turbidites and taphonomically-modified faunas. Mar. Micropaleontol. 148, 65–77. doi:10.1016/j.marmicro.2019.03.008

Hayward, B.W., Triggs, C.M., 2016. Using multi-foraminiferal-proxies to resolve the paleogeographic history of a lower miocene subduction-related, sedimentary basin (waitemata basin, new zealand). Journal of Foraminiferal Research 46, 285–313. doi:10.2113/gsjfr.46.3.285

Huang, T.-H., Chen, C.-T.A., Zhang, W.-Z., Zhuang, X.-F., 2015. Varying intensity of Kuroshio intrusion into Southeast Taiwan Strait during ENSO events. Continental Shelf Research 103, 79–87. doi:10.1016/j.csr.2015.04.021

Huh, C.-A., Lin, H.-L., Lin, S., Huang, Y.-W., 2009. Modern accumulation rates and a budget of sediment off the Gaoping (Kaoping) River, SW Taiwan: A tidal and flood dominated depositional environment around a submarine canyon. Journal of Marine Systems 76, 405–416. doi:10.1016/j.jmarsys.2007.07.009

Huh, C.-A., Su, C.-C., Liang, W.-T., Ling, C.-Y., 2004. Linkages between turbidites in the southern Okinawa Trough and submarine earthquakes. Geophys. Res. Lett. 31. doi:10.1029/2004GL019731

Huh, C.-A., Su, C.-C., Wang, C.-H., Lee, S.-Y., Lin, I.-T., 2006. Sedimentation in the Southern Okinawa Trough — Rates, turbidites and a sediment budget. Mar. Geol. 231, 129–139. doi:10.1016/j.margeo.2006.05.009

Hung, J.J., Lin, C.S., Hung, G.W., Chung, Y.C., 1999. Lateral Transport of Lithogenic Particles from the Continental Margin of the Southern East China Sea. Estuar. Coast. Shelf Sci. 49, 483–499. doi:10.1006/ecss.1999.0520

Ikehara, K., Kanamatsu, T., Usami, K., 2022. Possible Tsunami-Induced Sediment Transport From Coral Reef to Deep Sea Through Submarine Canyons on the Southern Ryukyu Forearc, Japan. Front. Earth Sci. 10. doi:10.3389/feart.2022.753583

Jan, S., Chen, C.-C., Tsai, Y.-L., Yang, Y.J., Wang, J., Chern, C.-S., Gawarkiewicz, G., Lien, R.-C., Centurioni, L., Kuo, J.-Y., 2011. Mean structure and variability of the cold dome northeast of taiwan. oceanog. 24, 100–109. doi:10.5670/oceanog.2011.98

Jones, R.W., 2013. Foraminifera and their Applications. Cambridge University Press, Cambridge. doi:10.1017/CBO9781139567619

Jorissen, F.J., de Stigter, H.C., Widmark, J.G.V., 1995. A conceptual model explaining benthic foraminiferal microhabitats. Mar. Micropaleontol. 26, 3–15. doi:10.1016/0377-8398(95)00047-X

Jorissen, F.J., Fontanier, C., Thomas, E., 2007. Chapter Seven Paleoceanographical Proxies Based on Deep-Sea Benthic Foraminiferal Assemblage Characteristics, in: Proxies in Late Cenozoic Paleoceanography, Developments in Marine Geology. Elsevier, pp. 263–325. doi:10.1016/S1572-5480(07)01012-3

Kao, S.J., Lin, F.J., Liu, K.K., 2003. Organic carbon and nitrogen contents and their isotopic compositions in surficial sediments from the East China Sea shelf and the southern Okinawa Trough. Deep Sea Res. Part II Top. Stud. Oceanogr 50, 1203–1217. doi:10.1016/S0967-0645(03)00018-3

Koyanagi, M., Masuda, Y., Takeshi, O., Shiro, H., 2010. Preliminary report on the Benthic foraminiferal assemblages in the west off Okinawa Island (GSJ Interim Report No. 51), Marine Geological and Geophysical Studies around Okinawa Islands -northwestern off of Okinawa Island- . National Advanced Industrial Science and Technology.

Lai, L.S.-H., Dorsey, R.J., Horng, C.-S., Chi, W.-R., Shea, K.-S., Yen, J.-Y., 2022. Extremely rapid up-and-down motions of island arc crust during arc-continent collision. Commun. Earth Environ. 3, 100. doi:10.1038/s43247-022-00429-2

Lee, I.-H., Lien, R.-C., Liu, J.T., Chuang, W., 2009a. Turbulent mixing and internal tides in Gaoping (Kaoping) Submarine Canyon, Taiwan. Journal of Marine Systems 76, 383–396. doi:10.1016/j.jmarsys.2007.08.005

Lee, I.-H., Wang, Y.-H., Liu, J.T., Chuang, W.-S., Xu, J., 2009b. Internal tidal currents in the Gaoping (Kaoping) Submarine Canyon. Journal of Marine Systems 76, 397–404. doi:10.1016/j.jmarsys.2007.12.011

Lee, S.-Y., Huh, C.-A., Su, C.-C., You, C.-F., 2004. Sedimentation in the Southern Okinawa Trough: enhanced particle scavenging and teleconnection between the Equatorial Pacific and western Pacific margins. Deep Sea Research Part I: Oceanographic Research Papers 51, 1769–1780. doi:10.1016/j.dsr.2004.07.008

Lee, T.-Y., Huang, J.-C., Lee, J.-Y., Jien, S.-H., Zehetner, F., Kao, S.-J., 2015. Magnified Sediment Export of Small Mountainous Rivers in Taiwan: Chain Reactions from Increased Rainfall Intensity under Global Warming. PLoS ONE 10, e0138283. doi:10.1371/journal.pone.0138283

Lehu, R., Lallemand, S., Hsu, S.-K., Babonneau, N., Ratzov, G., Lin, A.T., Dezileau, L., 2015. Deep-sea sedimentation offshore eastern Taiwan: Facies and processes characterization. Mar. Geol. 369, 1–18. doi:10.1016/j.margeo.2015.05.013

Levin, L.A., Gage, J.D., 1998. Relationship between oxygen, organic matter and the diversity of bathyal macrofauna. Deep Sea Research Part II 45, 129–163.

Liang, W.D., Tang, T.Y., Yang, Y.J., Ko, M.T., Chuang, W.S., 2003. Upper-ocean currents around Taiwan. Deep Sea Res. Part II Top. Stud. Oceanogr 50, 1085–1105. doi:10.1016/S0967-0645(03)00011-0

Lin, H.-L., Hsieh, H.-Y., 2007. Seasonal variations of modern planktonic foraminifera in the South China Sea. Deep Sea Res. Part II Top. Stud. Oceanogr 54, 1634–1644. doi:10.1016/j.dsr2.2007.05.007

Lin, H.-L., Liu, J.T., Hung, G.-W., 2005. Foraminiferal shells in sediment traps: Implications of biogenic particle transport in the Kao-ping submarine canyon, Taiwan. Continental Shelf Research 25, 2261–2272. doi:10.1016/j.csr.2005.09.001

Lin, H.-L., Sheu, D.D.-D., Yang, Y., Chou, W.-C., Hung, G.-W., 2011. Stable isotopes in modern planktonic foraminifera: Sediment trap and plankton tow results from the South China Sea. Mar. Micropaleontol. 79, 15–23. doi:10.1016/j.marmicro.2010.12.002

Lin, H.-L., 2014. The seasonal succession of modern planktonic foraminifera: Sediment traps observations from southwest Taiwan waters. Continental Shelf Research 84, 13–22. doi:10.1016/j.csr.2014.04.020

Liu, J.T., Hung, J.-J., Lin, H.-L., Huh, C.-A., Lee, C.-L., Hsu, R.T., Huang, Y.-W., Chu, J.C., 2009. From suspended particles to strata: The fate of terrestrial substances in the Gaoping (Kaoping) submarine canyon. Journal of Marine Systems 76, 417–432. doi:10.1016/j.jmarsys.2008.01.010

Liu, J.T., Lin, H.-L., Hung, J.-J., 2006. A submarine canyon conduit under typhoon conditions off Southern Taiwan. Deep Sea Research Part I: Oceanographic Research Papers 53, 223–240. doi:10.1016/j.dsr.2005.09.012

Ministry of Science and Technology – Republic of China, 2022. ODB – MOST [WWW Document]. Ocean Data Bank (ODB). URL https://www.odb.ntu.edu.tw/ (accessed 4.20.22).

Nayak, K., Lin, A.T.-S., Huang, K.-F., Liu, Z., Babonneau, N., Ratzov, G., Pillutla, R.K., Das, P., Hsu, S.-K., 2021. Clay-mineral distribution in recent deep-sea sediments around Taiwan: Implications for sediment dispersal processes. Tectonophysics 814, 228974. doi:10.1016/j.tecto.2021.228974

Nigam, R., Henriques, P.J., 1992. Planktonic percentage of foraminiferal fauna in surface sediments of the Arabian Sea (Indian Ocean) and a regional model for paleodepth determination. Palaeogeography, Palaeoclimatology, Palaeoecology 91, 89–98. doi:10.1016/0031-0182(92)90034-3

Olsen, A., Lange, N., Key, R.M., Tanhua, T., Álvarez, M., Becker, S., Bittig, H.C., Carter, B.R., Cotrim da Cunha, L., Feely, R.A., van Heuven, S., Hoppema, M., Ishii, M., Jeansson, E., Jones, S.D., Jutterström, S., Karlsen, M.K., Kozyr, A., Lauvset, S.K., Lo Monaco, C., Wanninkhof, R., 2019. GLODAPv2.2019 – an update of GLODAPv2. Earth Syst. Sci. Data 11, 1437–1461. doi:10.5194/essd-11-1437-2019

Parker, F.L., 1948. Foraminifera of the Continental Shelf from the Gulf of Maine to Maryland. Bulletin of the Museum of Comparative Zoology at Harvard College 100, 214–241.

Parker, F.L., 1954. Distribution of the Foraminifera in the northeastern Gulf of Mexico. Bulletin of the Museum of Comparative Zoology at Harvard College. 111, 451–588.

Poppe, L.J., Eliason, A.H., Fredericks, J.J., Rendigs, R.R., Blackwood, R.D., Polloni, C.F., 2000. Grain size analysis of marine sediments: methodology and data processing., in: USGS East-Coast Sediment Analysis: Procedures, Database, and Georeferenced Displays. US Geological Survey Open-File Report,00-358 (CD-ROM). United States Geological Survey.

Regenberg, M., Schroder, J.F., Jonas, A.S., Woop, C., Gorski, L., 2013. Weight loss and elimination of planktonic foraminiferal tests in a dissolution experiment. Journal of Foraminiferal Research 43, 406–414. doi:10.2113/gsjfr.43.4.406

Schiebel, R., Hemleben, C., 2017. Planktic foraminifers in the modern ocean, 2d ed. Springer Berlin Heidelberg, Berlin, Heidelberg. doi:10.1007/978-3-662-50297-6

Schmuker, B., 2000. The influence of shelf vicinity on the distribution of planktic foraminifera south of Puerto Rico. Mar. Geol. 166, 125–143. doi:10.1016/S0025-3227(00)00014-1

Schönfeld, J., Alve, E., Geslin, E., Jorissen, F., Korsun, S., Spezzaferri, S., 2012. The FOBIMO (FOraminiferal BIo-MOnitoring) initiative?Towards a standardised protocol for soft-bottom benthic foraminiferal monitoring studies. Mar. Micropaleontol. 94–95, 1–13. doi:10.1016/j.marmicro.2012.06.001

Schröder-Adams, C.J., Boyd, R., Ruming, K., Sandstrom, M., 2008. Influence of sediment transport dynamics and ocean floor morphology on benthic foraminifera, offshore Fraser Island, Australia. Mar. Geol. 254, 47–61. doi:10.1016/j.margeo.2008.05.002

Schröeder, C.J., Scott, D.B., Medioli, F.S., 1987. Can smaller benthic foraminifera be ignored in paleoenvironmental analyses? Journal of Foraminiferal Research 17, 101–105. doi:10.2113/gsjfr.17.2.101

Seismological Center – Republic of China, 2022. Central Weather Bureau - Seismological Center [WWW Document]. Seismic Activity. URL https://scweb.cwb.gov.tw/en-us/earthquake/data (accessed 4.20.22).

Sen Gupta, B.K., Machain-Castillo, M.L., 1993. Benthic foraminifera in oxygen-poor habitats. Mar. Micropaleontol. 20, 183–201. doi:10.1016/0377-8398(93)90032-S

Sugawara, D., Minoura, K., Nemoto, N., Tsukawaki, S., Goto, K., Imamura, F., 2009. Foraminiferal evidence of submarine sediment transport and deposition by backwash during the 2004 Indian Ocean tsunami. Island Arc 18, 513–525. doi:10.1111/j.1440-1738.2009.00677.x

Su, C.-C., Huh, C.-A., 2002. 210Pb, 137Cs and 239,240Pu in East China Sea sediments: sources, pathways and budgets of sediments and radionuclides. Mar. Geol. 183, 163–178. doi:10.1016/S0025-3227(02)00165-2

Su, C.-C., Tseng, J.-Y., Hsu, H.-H., Chiang, C.-S., Yu, H.-S., Lin, S., Liu, J.T., 2012. Records of submarine natural hazards off SW Taiwan. Geological Society, London, Special Publications 361, 41–60. doi:10.1144/SP361.5

Tapia, R., Ho, S.L., Wang, H.-Y., Groeneveld, J., Mohtadi, M., 2022. Contrasting vertical distributions of recent planktic foraminifera off Indonesia during the southeast monsoon: implications for paleoceanographic reconstructions. doi:10.5194/bg-2021-329

Uchida, J.-I., Fujiwara, O., Hasegawa, S., Kamataki, T., 2010. Sources and depositional processes of tsunami deposits: Analysis using foraminiferal tests and hydrodynamic verification. Island Arc 19, 427–442. doi:10.1111/j.1440-1738.2010.00733.x

Uchio, T., 1960. Ecology of living benthonic foraminifera from the San Diego, California, area. Cushman Foundation for Foraminiferal Research, Special Publication 1–72.

Usami, K., Ikehara, K., Jenkins, R.G., Ashi, J., 2017. Benthic foraminiferal evidence of deep-sea sediment transport by the 2011 Tohoku-oki earthquake and tsunami. Mar. Geol. 384, 214–224. doi:10.1016/j.margeo.2016.04.001

Usami, K., Ikehara, K., Kanamatsu, T., Kioka, A., Schwestermann, T., Strasser, M., 2021. The Link Between Upper-Slope Submarine Landslides and Mass Transport Deposits in the Hadal Trenchs, in: Sassa, K., Mikoš, M., Sassa, S., Bobrowsky, P.T., Takara, K., Dang, K. (Eds.), Understanding and Reducing Landslide Disaster Risk: Volume 1 Sendai Landslide Partnerships and Kyoto Landslide Commitment, ICL Contribution to Landslide Disaster Risk Reduction. Springer International Publishing, Cham, pp. 361–367. doi:10.1007/978-3-030-60196-6_26

van der Zwaan, G.J., Duijnstee, I.A.P., den Dulk, M., Ernst, S.R., Jannink, N.T., Kouwenhoven, T.J., 1999. Benthic foraminifers: proxies or problems? Earth-Science Reviews 46, 213–236. doi:10.1016/S0012-8252(99)00011-2

van der Zwaan, G.J., Jorissen, F.J., de Stigter, H.C., 1990. The depth dependency of planktonic/benthic foraminiferal ratios: Constraints and applications. Mar. Geol. 95, 1–16. doi:10.1016/0025-3227(90)90016-D

van Hinsbergen, D.J.J., Kouwenhoven, T.J., van der Zwaan, G.J., 2005. Paleobathymetry in the backstripping procedure: Correction for oxygenation effects on depth estimates. Palaeogeography, Palaeoclimatology, Palaeoecology 221, 245–265. doi:10.1016/j.palaeo.2005.02.013

van Marle, L.J., van Hinte, J.E., Nederbragt, A.J., 1987. Plankton percentage of the foraminiferal fauna in seafloor samples from the Australian-Irian Jaya continental margin, eastern Indonesia. Mar. Geol. 77, 151–156. doi:10.1016/0025-3227(87)90089-2

Water Resources Agency – Republic of China, 2022. Water Resources Agency, MOEA [WWW Document]. Water Resources Agency. URL https://eng.wra.gov.tw/ (accessed 4.20.22).

Weinkauf, M.F.G., Milker, Y., 2018. The effect of size fraction in analyses of benthic foraminiferal assemblages: A case study comparing assemblages from the >125 and >150 µm size fractions. Front. Earth Sci. 6. doi:10.3389/feart.2018.00037

Wilcoxon, J.A., 1964. Contributions from the Cushman Foundation for Foraminiferal Research Distribution of foraminifera off the southern Atlantic coast of the United. Contributions from the Cushman Foundation for Foraminiferal Research 15, 1, 24.

Table 1. Correlation coefficient (Spearman rank) between foraminifera data and environmental parameters. Depth: Water depth (m); %Sand: grain size >63 µm; TOC: TOC content; Temp.: Temperature (ºC) 0–400 m; Sal.: Salinity 0–400 m; Fluo.: Fluorescence 0–400 m; Surface D.O.: Dissolved oxygen 0–400 m; Bottom D.O.: bottom water dissolved oxygen; Planktic: Planktic foraminiferal abundance; Benthic: Benthic foraminiferal abundance.

	Sedimentary			Hydrography					Foraminifera		
	Depth	%Sand	TOC	Temp.	Sal.	Fluo.	Surface DO	Bottom DO	%P	Benthic	Planktic
%P	0.567 ***	-0.199	0.255 *	0.155	0.332 **	-0.488 ***	0.156	-0.354 **	–		
Benthic	-0.650 ***	0.226	-0.389 **	0.107	—	0.250 *	-0.221	0.416 ***	-0.480 ***	–	
Planktic	0.231 *	-0.106	0.098	0.134	0.088	-0.366 **	0.079	-0.126	0.756 ***	0.125	–

Note. * p < .05, ** p < .01, *** p < .001

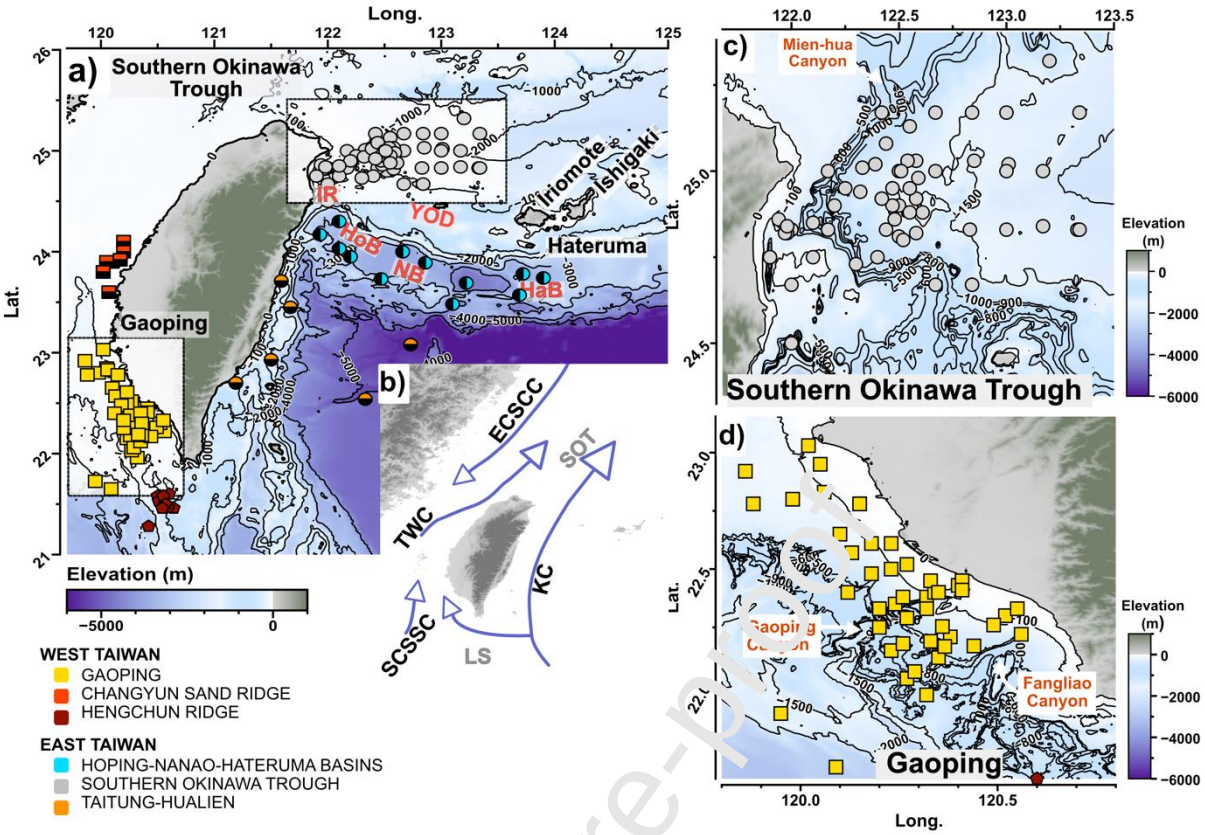

Figure 1. a) Bathymetric chart depicting the location of surface sediment samples analyzed in this study; the inset (b) is a schematic illustrating the location of the Southern Okinawa Trough (SOT) and Luzon Strait (LS) sectors and the main surface currents offshore Taiwan, namely Kuroshio Current (KC), South China Sea Surface Current (SCSSC), Taiwan Warm Current (TWC) and East Coastal China Sea Current (ECSCC). The study sites were separated into two primary areas according to their longitude, West Taiwan (> 121º E) and East Taiwan (< 121º E). East Taiwan is comprised of the sectors of Southern Okinawa Trough, Hoping-Nanao-Hateruma Basins, and Taitung-Hualien Slope, while West Taiwan is comprised of the sectors of Gaoping, Changyun Sand Ridge, and Hengchun Ridge. Panels (c) and (d) are close-ups of the sectors depicted in (a). The location of the Hoping (HoB), Nanao (NB) and Hateruma Basins (HaB), Ilan Ridge (IR), Yonaguni Depression (YoD), and the Ryukyu Islands (Hateruma, Iriomote, and Ishigaki) are depicted in (a); the Mien-Hua Canyon in (b); and the Gaoping and Fangliao Canyon in (c).

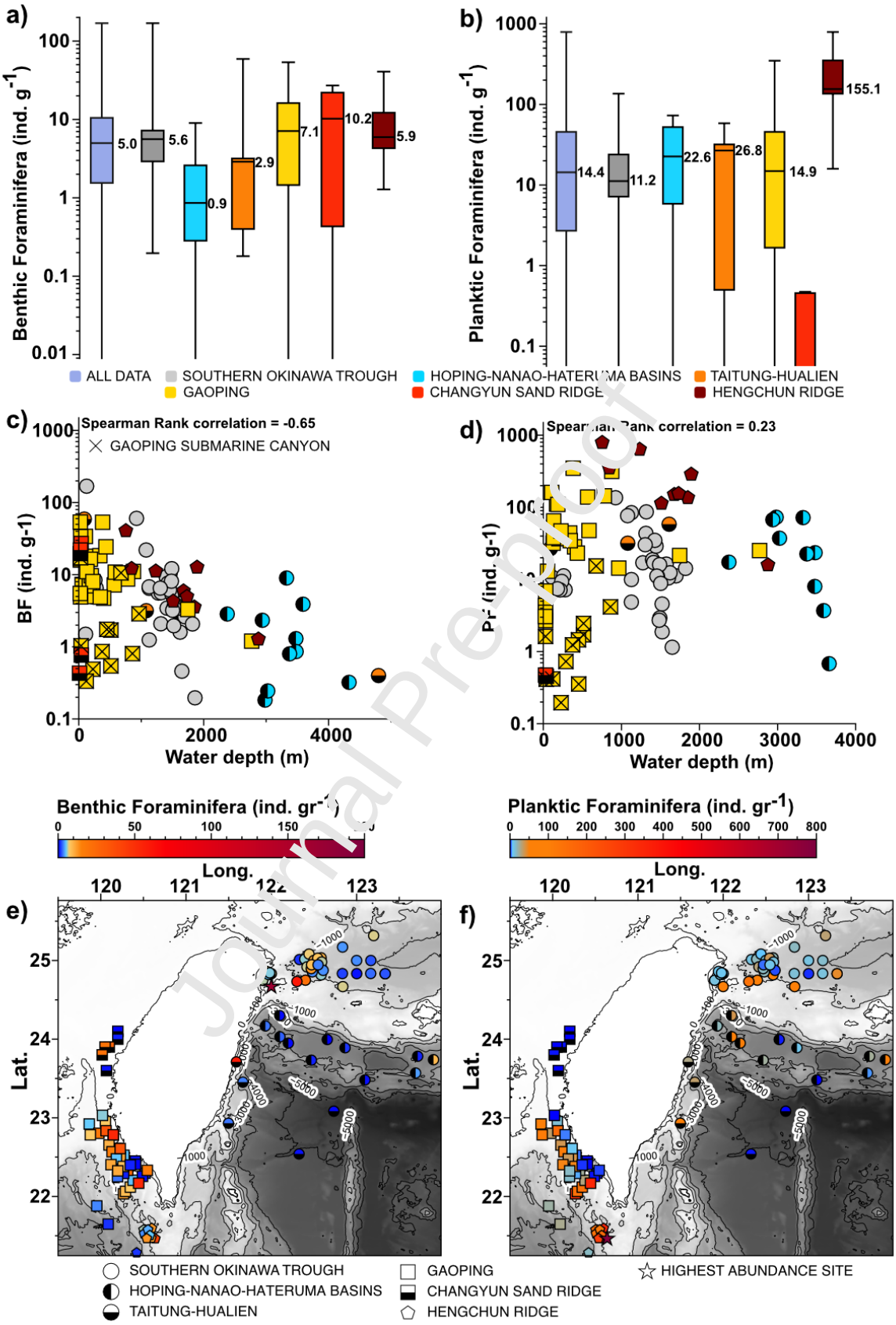

Figure 2. Box plots depicting the abundance of benthic (a) and planktic foraminifera (b) (>125 µm) off Taiwan for the entire dataset and by sectors. In each box plot, whiskers mark the maximum

and minimum values, while the number represents the median value. Comparison of the abundances of (c) benthic and (d) planktic foraminifera as a function of bathymetry. Overall, the abundances of benthic foraminifera decrease with depth while the abundances of planktic foraminifera increase. The stations located in the Gaoping and Fangliao submarine canyons are marked (x). The spatial distribution of the abundances of (e) benthic and (f) planktic foraminifera (>125 μm) off Taiwan shows that high abundances of benthic foraminifera are mostly restricted to shallow sites close to the coast while high abundances of planktic foraminifera occur at deep sites. Symbols represent the different sectors considered in this study; stars depict the station with the highest abundance; colors depict the abundance at each site.

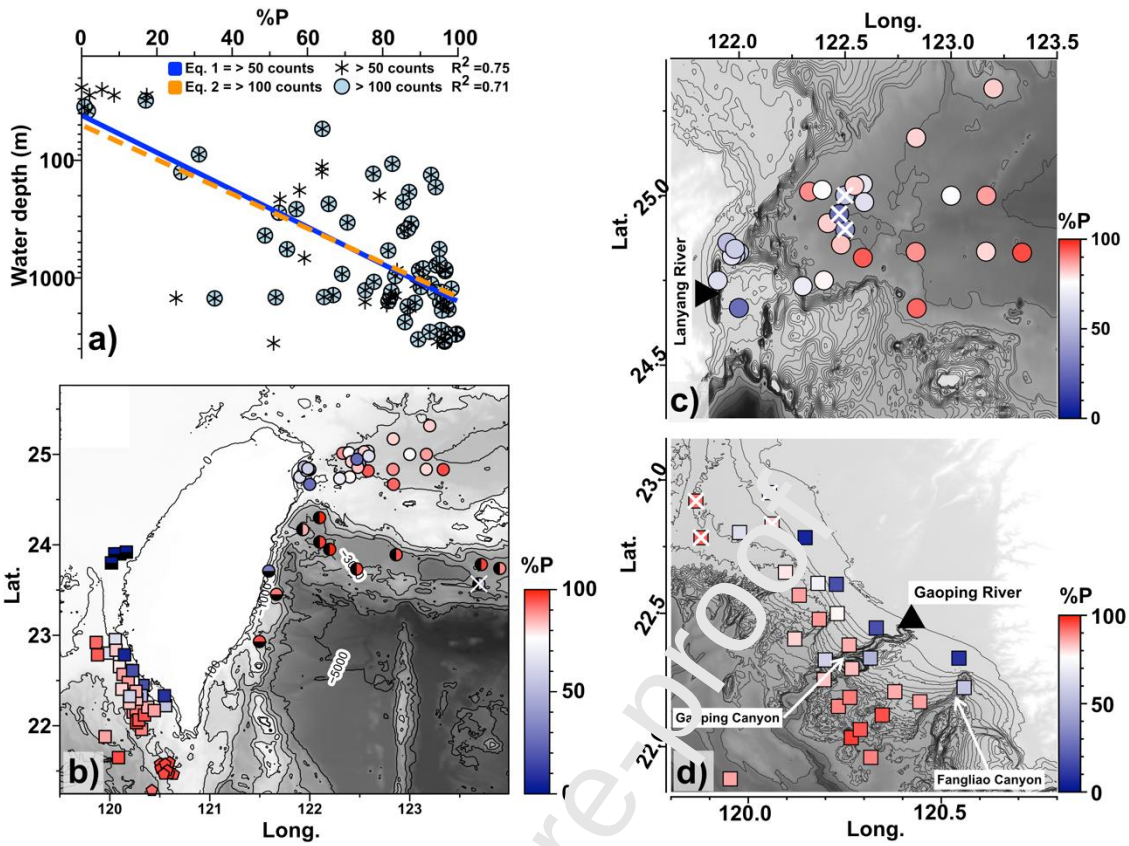

Figure 3. (a) Comparison of the relationship between %P and water depth considering samples with >50 counts (n = 88) (asterisk) and ≥ 100 counts (n = 67) (filled circles). (b) Bathymetric chart off Taiwan showing the spatial distribution of %P values at stations with (a) all >50 foraminifera counts (>125 µm; n = 88), (c) the Southern Okinawa Trough (SOT) and (d) Gaoping sector. Black lines and gray shading depict the seafloor bathymetry; bathymetric lines in c and d show the elevation in 50 m intervals. Stations where %P data lay outside of the 95% prediction range of the regression are marked (x) (see text for details).

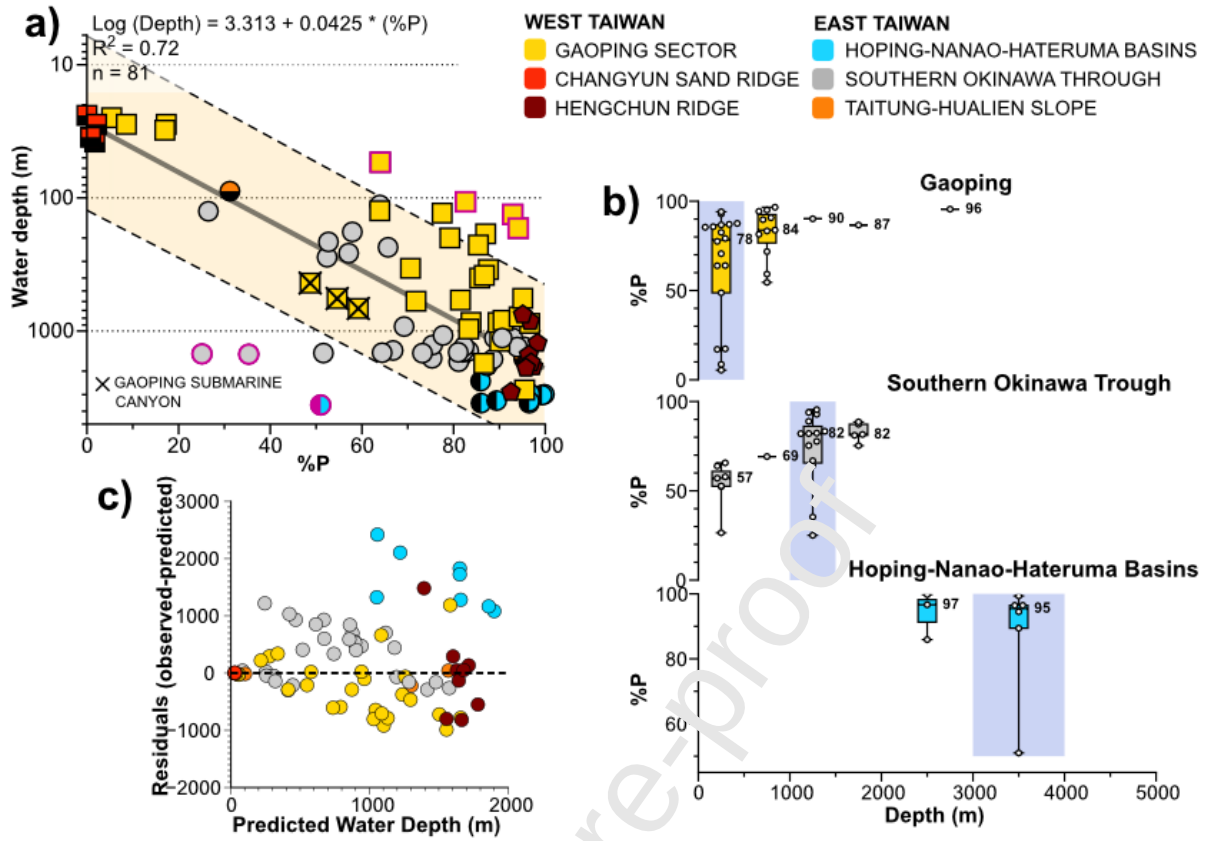

Figure 4. (a) Regression of %P against water depth off Taiwan (n= 81). The yellow shaded area depicts the prediction bounds (95%), while stations located in the Gaoping Submarine Canyon are marked by the symbol (x). The reported regression equation only considers data points within the 95% prediction bounds (2σ) of the regression model. Data > 2σ are considered outliers and marked in violet. (b) %P variability by depth range for the sectors of Gaoping (yellow), Southern Okinawa Trough (gray), and Hoping-Nanao-Hateruma Basins (turquoise). The data are grouped by depth bin of 500 m for Gaoping and Southern Okinawa Trough and 1000 m for Hoping-Nanao-Hateruma Basins. Blue boxes depict the depth bin with the largest data dispersion. The numbers depict the median value for the depth bin. (c) Residuals of the Taiwan calibration (excluding the outliers marked in panel a) show that the bathymetry estimates may be over- or underestimated by ~1000 m for most sectors.

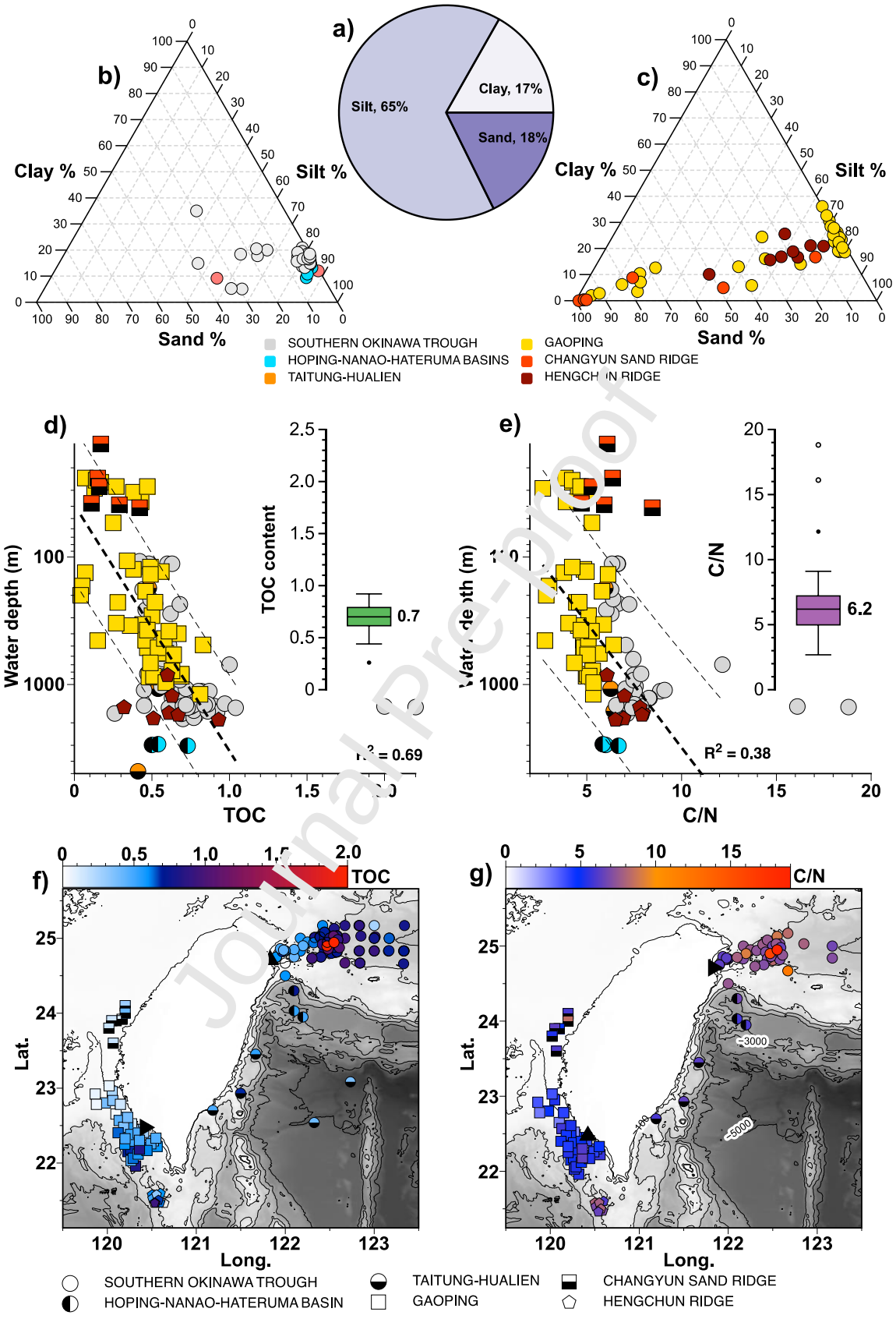

Figure 5. Grain size distribution of (a) the average value of the entire dataset off Taiwan and by site in (b) East Taiwan and (c) West Taiwan. Relationships between water depth and bulk

sedimentological parameters, namely (d) Total Organic Carbon (TOC) content and (e) C/N ratio. The TOC content has a stronger correspondence with water depth than the C/N ratio. The number in the box plots represents the median value of TOC and the C/N ratio, respectively. Outliers were not considered in the correlation. River mouths i.e., Lanyang (north) and Gaoping (south) are indicated by triangles.

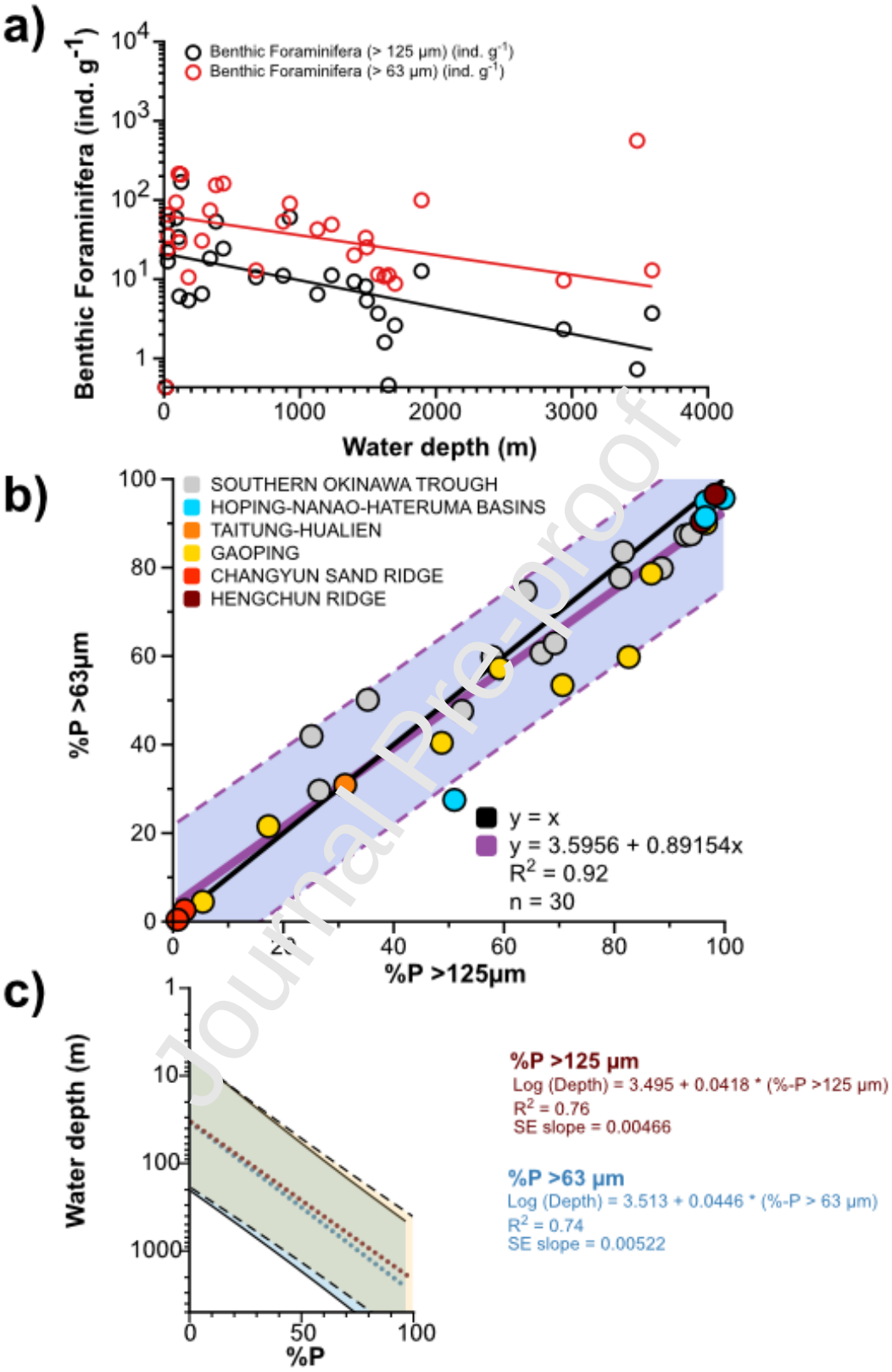

Fig 6. Assessment of the effect of size fraction selection on the abundances, %P index and its relationship with water depth. a) The abundances of benthic foraminifera from the size fraction of >63 μm and >125 μm both decrease with water depth. b) The %P values calculated from the size fraction of >63 μm and >125 μm are highly correlated (R^2 =0.92), and c) The regression between %P and water depth is insensitive to the size fraction selection, as indicated by comparable regression lines and their respective coefficient of determination (R^2) for the size fraction of >63 and >125 μm.

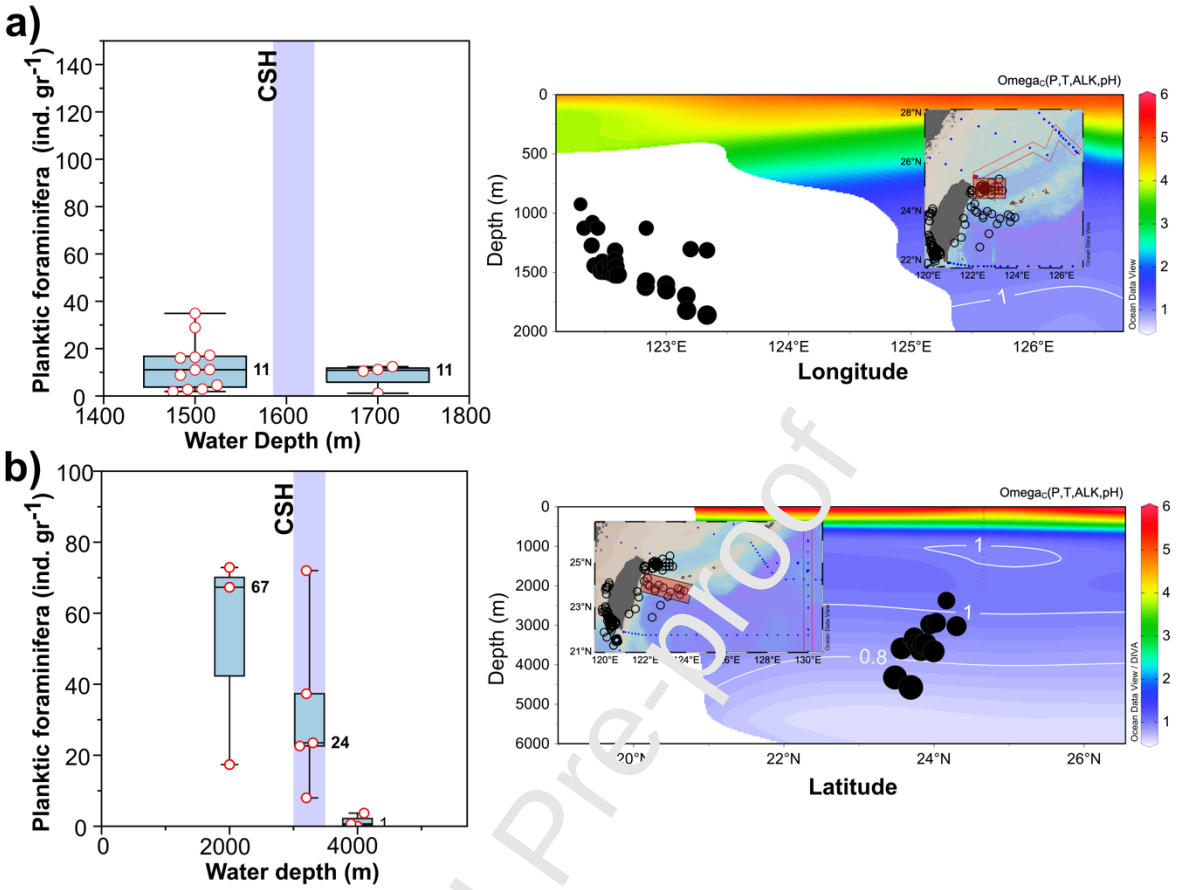

Figure 7. Box plots showing the distribution and average value of foraminiferal tests in sediments above and below the Carbonate Saturation Horizon (CSH; Ω_c = 1; indicated by blue shaded bars) for (a) the Southern Okinawa Trough and (b) the Nanao-Hoping-Hateruma Basins. Similar (dissimilar) values above and below the calculated saturation horizon suggest a small (large) effect of carbonate dissolution on the abundance of planktic foraminifera. The Calcite Saturation Horizon was calculated using the GLODAPv.2 database (Olsen et al., 2019) for Ocean Data View (Schlitzer, 2002). The right panels show the oceanographic sections selected for the Calcite Saturation Horizon calculation and the position of the stations in the Southern Okinawa Trough (upper panel) and Nanao-Hoping-Hateruma Basins (lower panel). Red shaded boxes in the insets depict the sectors while the red boxes depict the oceanographic section used in the calculation of Ω_c.

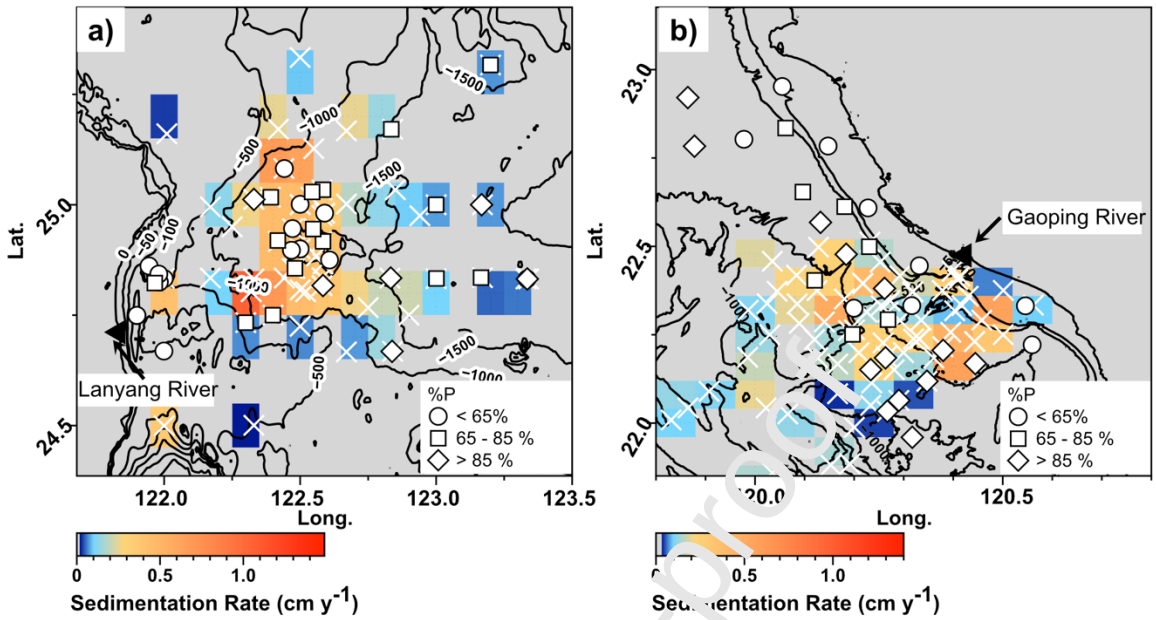

Figure 8. Distribution of %P in (a) Southern Okinawa Trough and (b) Gaoping sectors plotted on top of sedimentation rate estimates based on ^{210}Pb data from Huh et al., 2006, 2009 and Lee et al., 2004. In the Southern Okinawa Trough stations with low (<65%; circles) and moderate (65–85%; squares) %P values concentrate in the sector of high sedimentation rate, while stations with high %P values (>85%) mostly occurs outside of the high sedimentation rate areas. In contrast, in the Gaoping sector, low (<65%; circles) and moderate (65–85%; squares) %P values are associated with submarine canyons where the sedimentation rates are low due to downslope flushing of sediments. Symbols depict the locations of the %P stations (circle, square, and diamond), ^{210}Pb stations (x), and the Lanyang and Gaoping rivers (triangles).

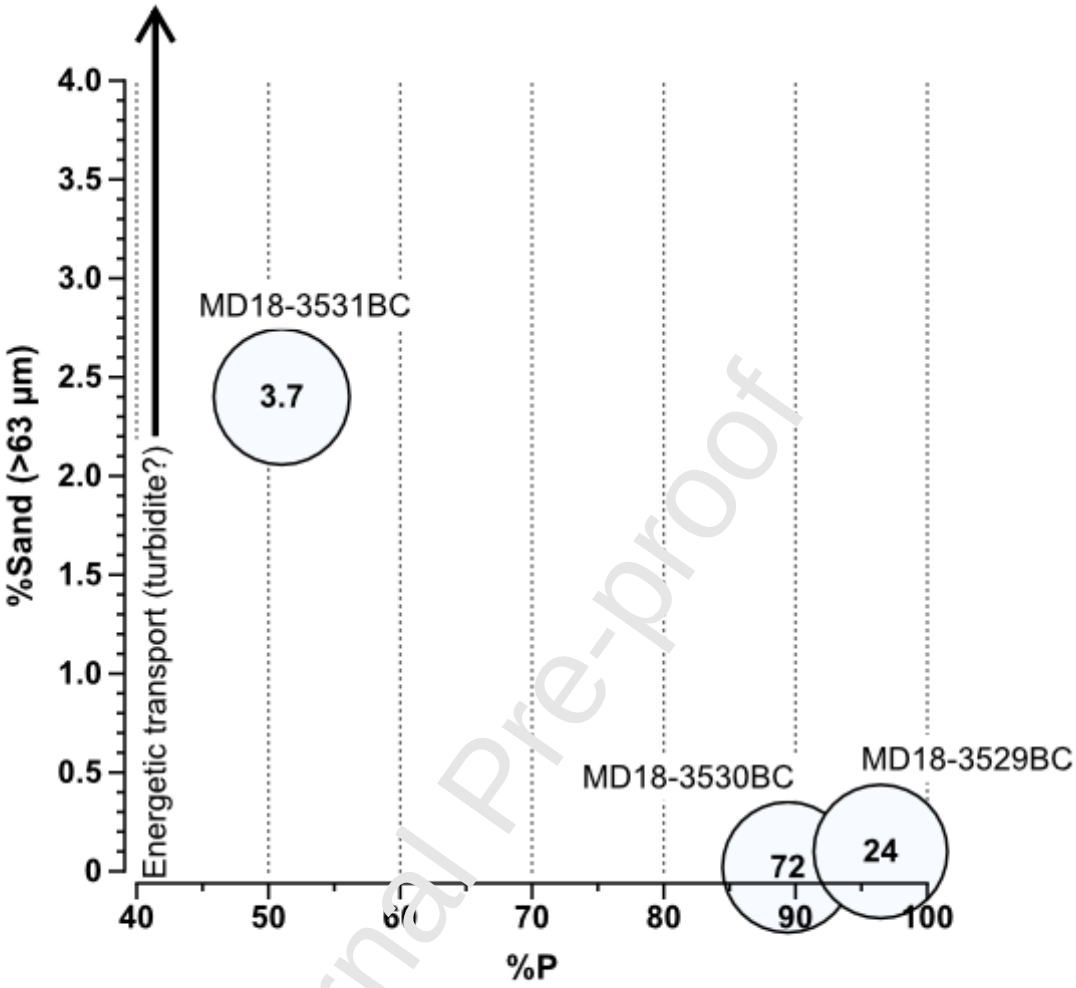

Figure 9. Relationship between %Sand, %P, and planktic foraminiferal abundance at three sites in the Hateruma basin. Number in the circles indicates planktic foraminiferal abundance. The %P values at sites MD18-3529BC (3480 m), MD18-3530BC (3326 m), and MD18-3531BC (3590 m) differ substantially despite being located at similar water depths. The low abundance of planktic foraminifera and high %sand (>63 microns) suggest a possible influence of carbonate dissolution and/or the input of allochthonous sediment due to downslope transport (see section 4.3.2 for details).

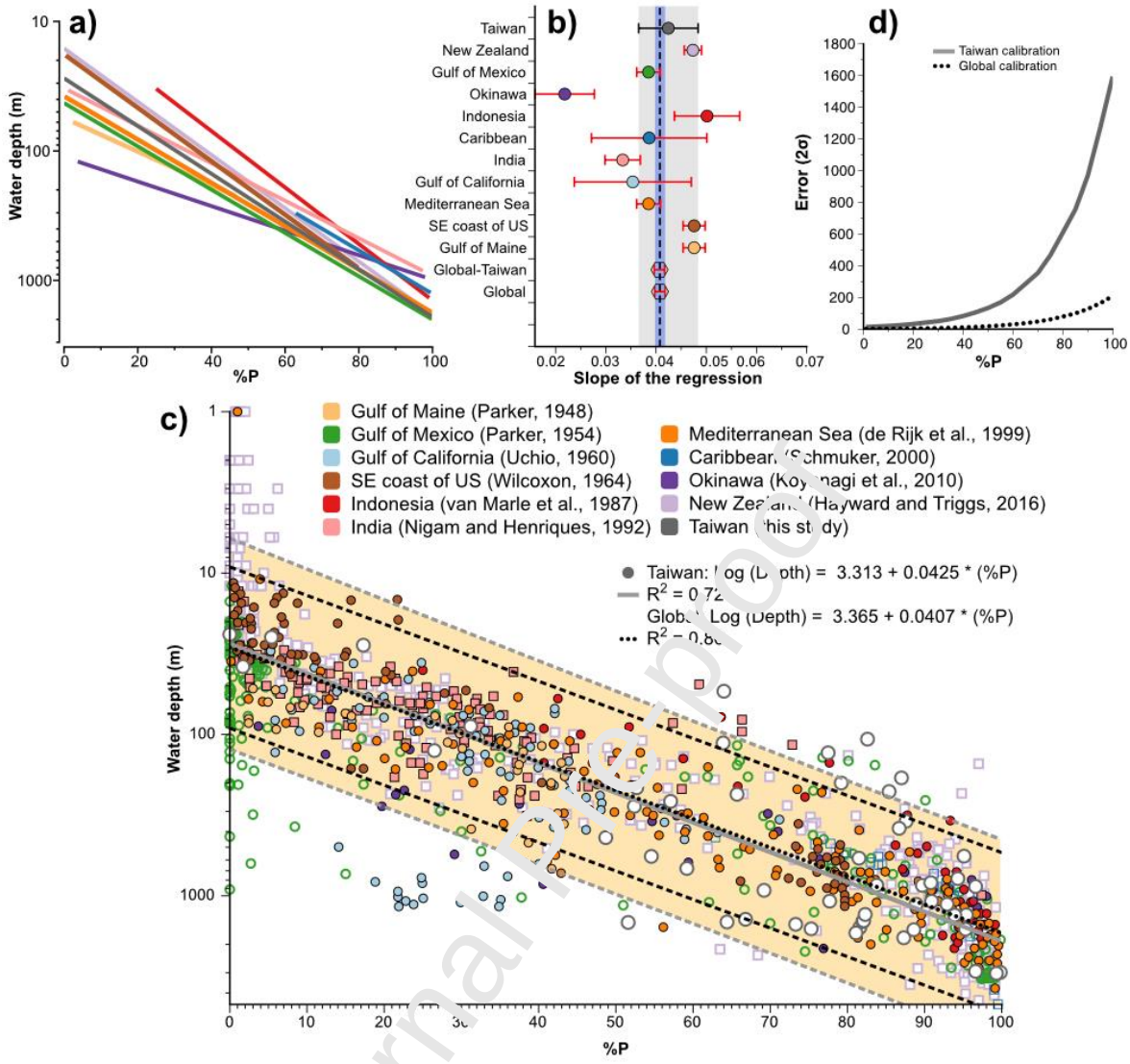

Figure 10. (a) Comparison of the %P-water depth relationships from different regions indicates regional differences in the regression lines. All regional datasets show a general positive relationship between %P and water depth, albeit with varying degrees of scatter. b) Slopes of the regression for each sector (± 95 % confidence interval). The dashed line indicates the slope of the global compilation excluding the dataset from Taiwan (± 95% confidence interval of the mean slope; Global – Taiwan). Error bars represent 2σ standard error of the slope, and shaded areas represent the 2σ error for Taiwan (gray) and Global – Taiwan (blue) datasets, respectively. (c) The regression based only on data offshore Taiwan (n = 81 after outlier removal; see Fig. 4) agrees well with that based on the global compilation (n = 1077; n = 1004 after outlier removal) obtained by combining all the regional datasets. Solid lines depict the regression equation, while the dashed lines depict the 95% prediction bounds. The data sets from Uchio (1960) and Wilcoxon (1964) were digitalized from van der Zwaan et al. (1990), while the dataset from Rijk et

al. (1999) was digitalized from the original article. Data digitization was performed using PlotDigitizer (https://plotdigitizer.com).

10. Supplementary Information

Table S1. Details of the core sites used in this study. The sites are divided into East Taiwan, which comprises the Southern Okinawa Trough (1), Nanao-Hoping-Hateruma Basins (2), and Taitung-Hualien (3). The area of West Taiwan consists of the Gaoping (4), Changyun Sand Ridge (5), and Hengchun Ridge (6) sectors.

>>> Associated Excel File <<<<<

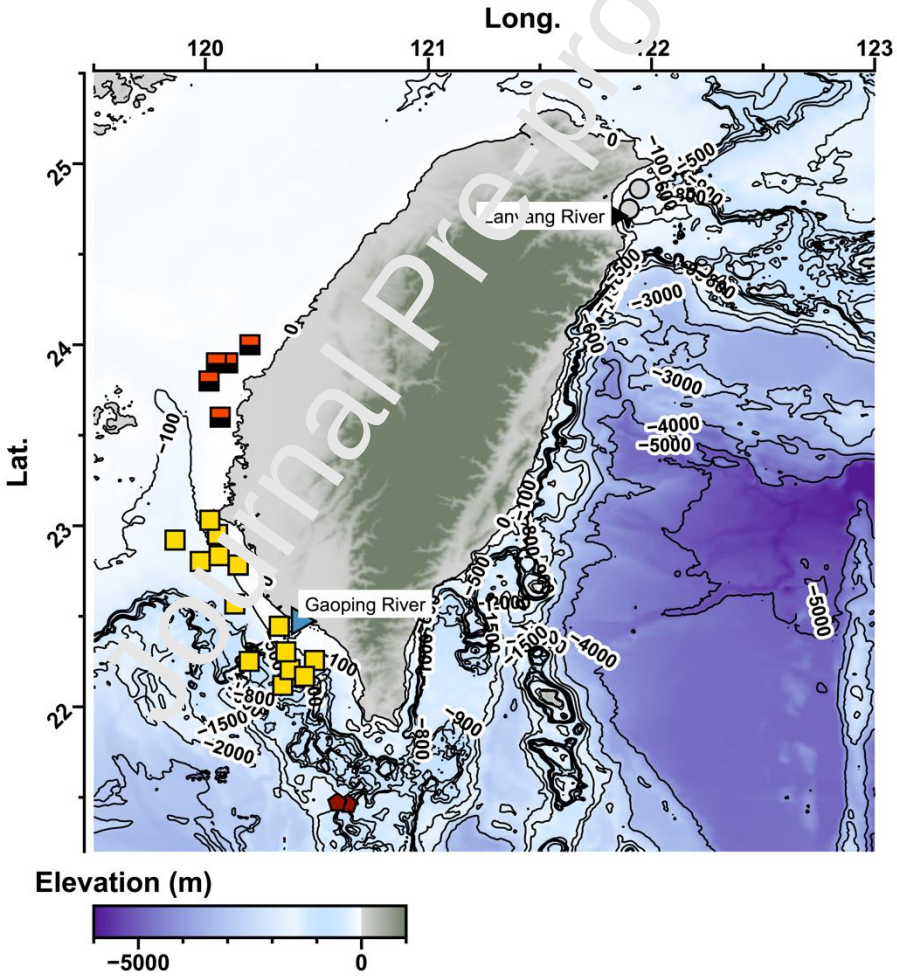

Fig. S1 Location of the stations where sediments contain >20% of sand (>63 μm) content. Triangles depict the location of the Lanyang River (black triangle) and Gaoping River (blue triangle).

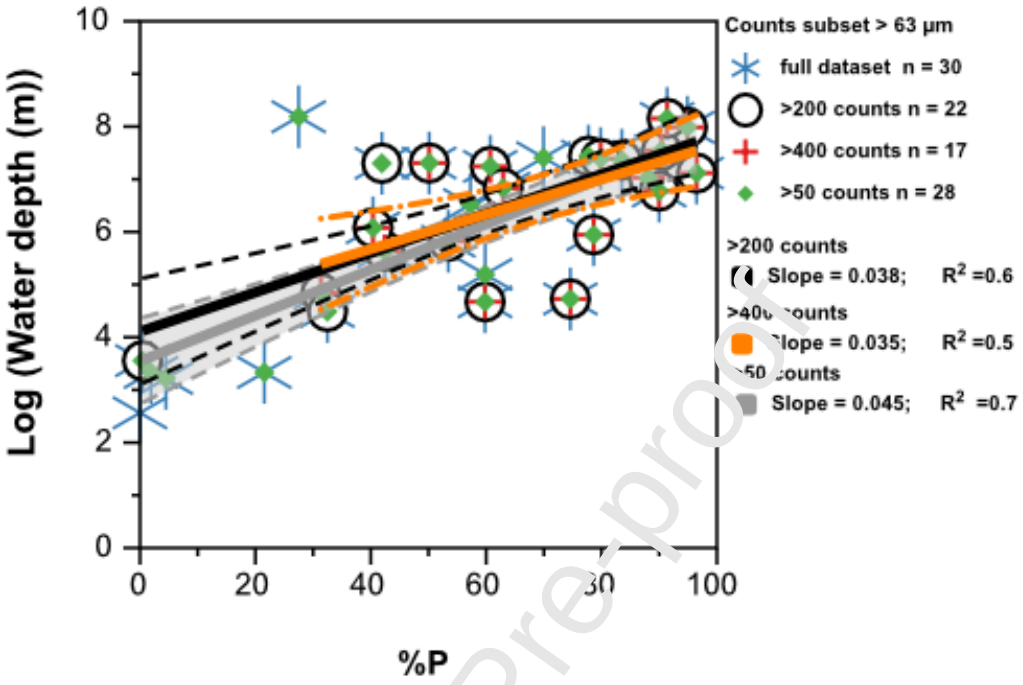

Fig. S2 The assessment of the effect of the count threshold, i.e., >50, >200, and >400 count per sample, on the %P-water depth relationship was performed on the 63 µm subset (30 samples). The regression lines for different count thresholds agree within error (dashed lines; 95% prediction bounds). The coefficient of determination (R2) of the regressions decreases with increasing count threshold, likely due to decreasing number of data points that are included in the regression. This implies that whilst a higher count threshold may yield stronger statistical representativeness of the %P value, the resultant smaller data set leads to a less reliable regression model.

Fig. S3 Microphotographs of shallow water benthic foraminifera in the surface sediments of the stations OR1-642-BC22 (%P = 81) and OR1-0715-20 (%P = 90), of genus *Amphistegina* (1,2,3), *Calcarina* (4), *Neorotalia* (5) and *Elphidium* (6,7).

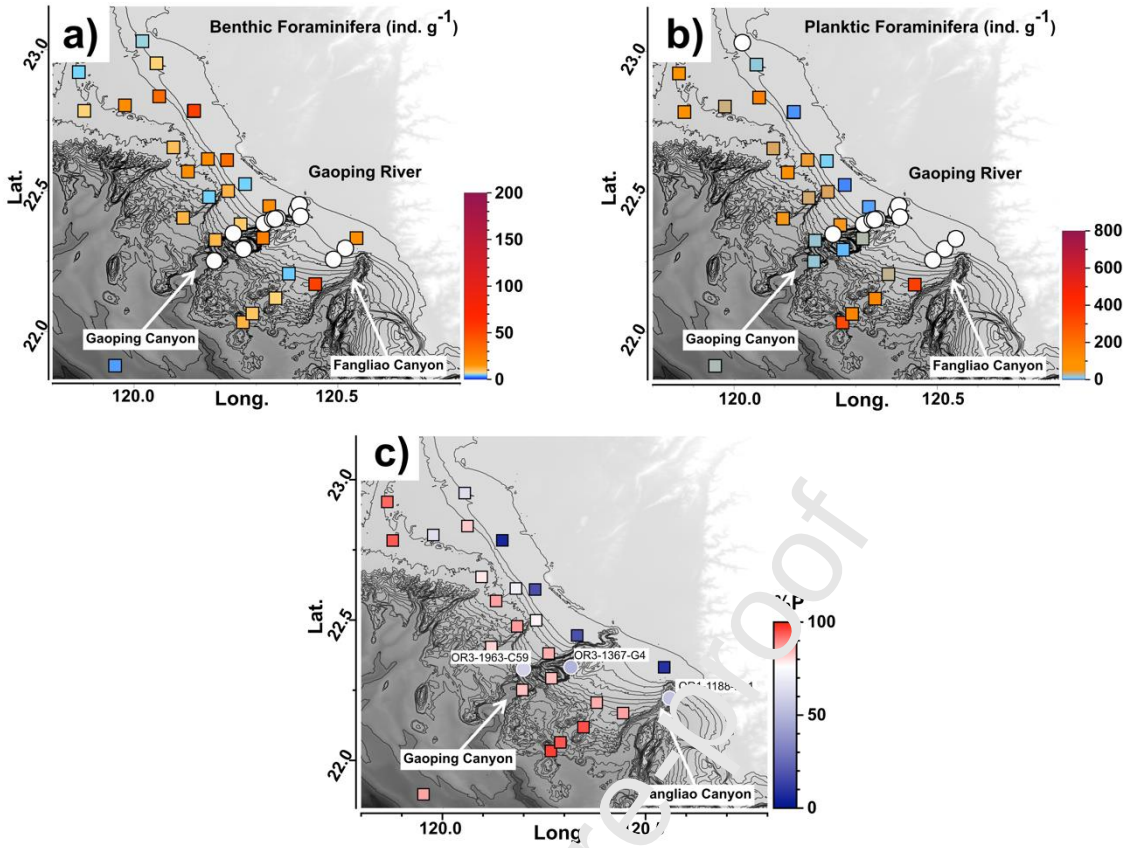

Fig. S4 Distribution of (a) benthic and (b) planktic foraminiferal abundance in the Gaoping sector. Low abundances characterize sites in the submarine canyons (< 3 ind. g^{-1}; white circles), while the abundances are higher elsewhere. (c) %P values at sites in the canyons (circles) are relatively low for their bathymetric range. Black lines and gray shading depict the seafloor bathymetry, and bathymetric lines show the elevation in 50 m intervals.

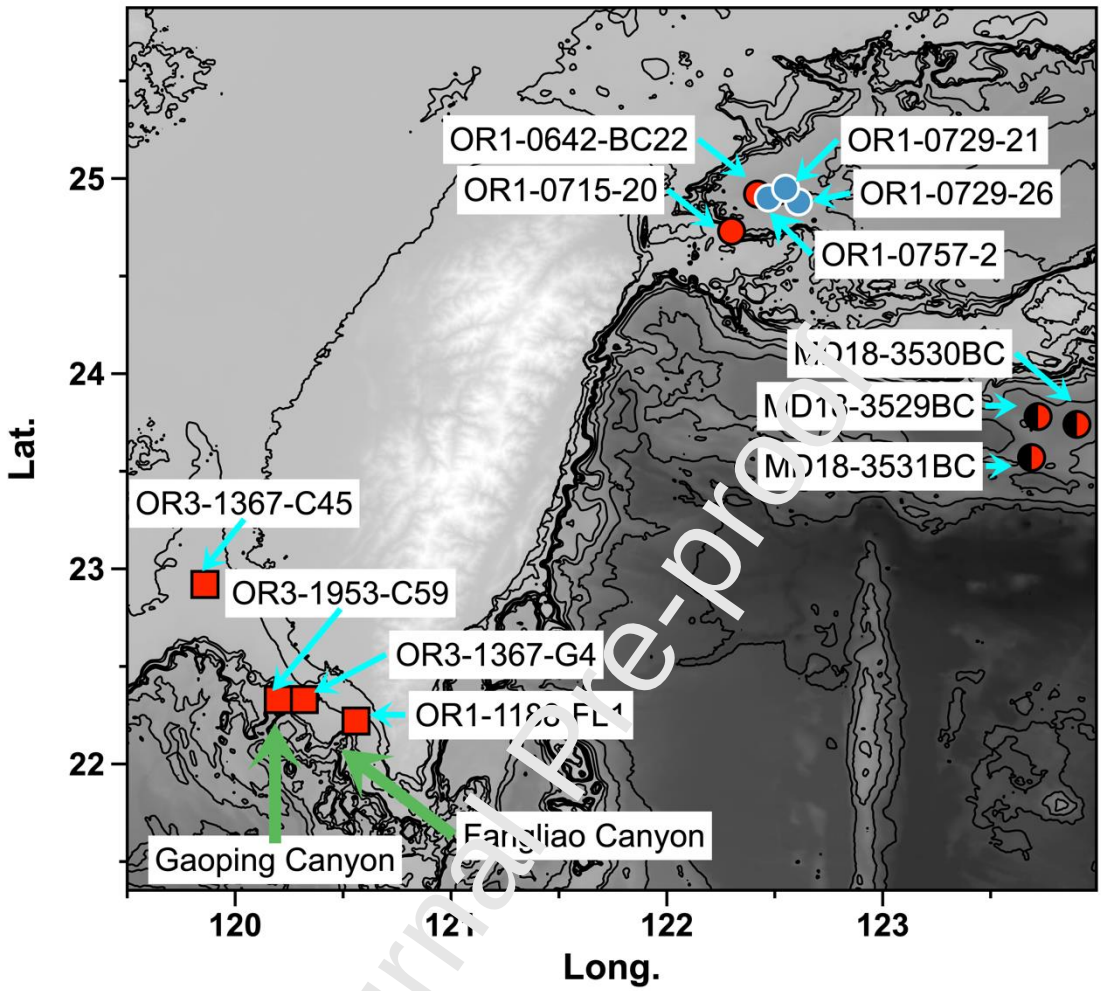

Fig. S5 Location of the foraminifera index stations (red symbols) mentioned and discussed in the manuscript, i.e., OR1-0642-BC22, OR1-0715-20 in the Southern Okinawa Trough, MD18-3531BC, MD18-3529BC, MD18-3530BC in Hoping-Nanao-Hateruma Basins, OR1-1188-FL1 OR3-1367-C4, OR3-1420-C8, and OR3-1367-C45 in the Gaoping area, as well as stations with high TOC and C/N values (blue symbols), i.e., OR1-0729-21 and OR1-0729-26.

Table 1. Correlation coefficient (Spearman rank) between foraminifera data and environmental parameters. Depth: Water depth (m); %Sand: grain size >63 µm; TOC: TOC content; Temp.: Temperature (ºC) 0–400 m; Sal.: Salinity 0–400 m; Fluo.: Fluorescence 0–400 m; Surface D.O.: Dissolved oxygen 0–400 m; Bottom D.O.: bottom water dissolved oxygen; Planktic: Planktic foraminiferal abundance; Benthic: Benthic foraminiferal abundance.

	Sedimentary			Hydrography				Foraminifera		
	Depth	**%Sand**	**TOC**	**Temp.**	**Sal.**	**Fluo.**	**Surface DO**	**Bottom DO**	**%P**	**Benthic**	**Planktic**
%P	0.0567***	-0.199	0.255*	0.155	0.332	-0.488***	0.156	-0.354**	-		
Benthic	-0.650***	0.229	-0.389**	0.107	-	0.250*	-0.221	0.416**	-0.480***	-	
Planktic	0.231*	-0.106	0.098	0.134	0.088	-0.366**	-0.126	-0.126	0.756***	0.125	-

*Note. *p < 0.05, **p < .01, ***p< .00*

Declaration of Interest

The authors declare that they have no known competing financial interests or personal relationships that could have appeared to influence the work reported in this paper.

HIGHLIGHTS

- Foraminifera, grain size, TOC, and C/N data of 148 core-tops off Taiwan
- Bathymetry is the main driver of foraminiferal abundance
- Planktic foraminifera percentage (%P) is strongly correlated with seafloor bathymetry
- Lateral advection, carbonate dissolution, and downslope sediment transport affect %P
- %P a promising tool for paleo-bathymetry, -geohazard, and -oceanography studies